A Role for CLASPs in the Regulation of the Major Microtubule +TIP Complex Organizers, End-Binding Proteins

By

Ashley Dyan Grimaldi

Dissertation

Submitted to the Faulty of the

Graduate School of Vanderbilt University

In partial fulfillment of the requirements

For the degree of

DOCTOR OF PHILOSOPHY

in

Cell and Developmental Biology

August, 2014

Nashville, Tennessee

Approved:

Laura A. Lee, M.D., Ph.D.

Matthew J. Tyska, Ph.D.

Ryoma Ohi, Ph.D.

Matthew J. Lang, Ph.D.

Irina Kaverina, Ph.D.

To my loving a supportive parents, Deborah and Steve, who have guided and supported me throughout my life

and

To my sisters, Erica and Robyn, who have loved and stood by me in all that I have done

and

To my beloved dog, Kolby, who has been faithfully by my side throughout this long, but rewarding experience.

ACKNOWLEDGEMENTS

I would like to express my deep appreciation and gratitude to my advisor, Dr. Irina Kaverina, for her patience and for the mentorship she provided to me throughout my time here at Vanderbilt University. As the leader of the Kaverina lab, she helps us all to strive for scientific excellence and encourages us not to be afraid of a challenge. As a teacher and a mentor, she has taught me more about science and life than I could ever begin to give her credit for here.

I would also like to thank my committee members, Drs. Laura Lee, Matthew Tyska, Ryoma Ohi, and Matthew Lang for their support and leadership in the completion of my manuscript and doctoral work; I am a better scientist and stronger person thanks to their guidance. Additionally, thank you to the Department of Cell and Developmental Biology and the Interdisciplinary Graduate Program in the Biomedical and Biological Sciences for fostering a welcoming and unmatched educational setting in which to develop as a scientist and a student.

I would like to give a special thanks to my committee chair, Dr. Laura Lee, who has always gone above and beyond to help me feel secure within the Department of Cell and Developmental Biology. She welcomed me into her office many a time to listen to my dilemmas and always helped me to find the best solutions moving forward. I will

be forever grateful to Dr. Lee for her support and guidance in my decision to pursue teaching as a career.

The work presented in this dissertation was produced with the help of funding from NIH NIGMS grant RO1-GM078373-01 to I.K., and American Heart Association Grant-in-Aid 13GRNT16980096 to I.K., as well as American Heart Association Predoctoral Fellowship 12PRE12040153 to A.D.G.

I am extremely fortunate to have had the chance to work with such amazing colleagues at Vanderbilt and to make wonderful friendships here in Nashville. A special thank you to Chris for being the best lab mate and friend that I could have ever asked for. I am so glad that we had each other to lean on throughout this experience and I do not know what I will do without you in the coming years (it will be quite the adjustment). Thank you to Xiaodong Zhu for your friendship and counsel in lab. Your scientific knowledge is astounding and I will always remember your guidance in the completion of my work. To the rest of the Kaverina Lab, Justin (De-Shawn), Keyada (Chelsea), Nadia, Maria and Dmitry, thank you for your support, your friendship and for providing a welcome distraction from lab when needed.

The tremendous collaborative nature of science at Vanderbilt means that I also owe many thanks to other labs within the University. Thank you to the ladies of the Ohi lab (Emma, Sophia, and Jen) for teaching me about *in vitro* work and for always helping

me with questions about experiments or life in general. Also, thank you to the Tyska lab (especially Scott and Nathan) for always lending a helpful hand and sharing in the experience of graduate school. Thank you to Jeanne, of the Lee Lab, for your warm friendship and guidance in the navigation of graduate school; without your help, I may not have survived all in one piece.

I must acknowledge a couple of friendships that have meant the world to me during my time in Nashville. To Elaine and Michelle for being excellent friends during IGP and especially to Elaine for your continued friendship and love during these past few years. Alice (and Zara) and Sarah (and Guinevere), thank you for being my family in Nashville and for always being there for me (and Kolby) and giving me a much-needed escape from the world of science. Of course, I must thank the outstanding employees at Bellevue Animal Hospital for their help in taking care of Kolby over the past four years and for giving me piece of mind while away at Vanderbilt each day. To everyone not mentioned, I would like to thank you for being there for me throughout my time in graduate school; I truly appreciate your encouragement and I am grateful to each and every one of you.

Finally, I would like to thank my entire family (dogs and all) for their unwavering love and support over the past few years. Thank you for your guidance, for supporting me in my decisions, and for reminding me about what is truly important in life.

TABLE OF CONTENTS

LIST OF FIGURES

I. INTRODUCTION

II. CLASPs ARE REQUIRED FOR PROPER MICROTUBULE LOCALIZATION OF END-BINDING PROTEINS

CHAPTER I

INTRODUCTION

Microtubule Network

The cell is the basic structural and functional component of all living organisms and the smallest unit of life. Within cells, there are many organelles and structures that carry out diverse functions as well as provide regulation to the cell itself. One key structural and regulatory element is the cytoskeleton, which is comprised of three branches: actin, intermediate filaments, and microtubules. Together, the mechanical properties of these components provide shape and strength to the interior of the cell, hence the term cytoskeleton. Although the cytoskeleton provides a framework for the cell, it is quite dynamic in nature with the different polymers constantly remodeling and moving throughout the cell. The focus of this section will be on microtubules (MTs), their functions, and their associated regulatory proteins.

For many years, it was thought that the cytoskeleton only existed in eukaryotic cells and that this was one of the defining characteristics between eukaryotes and prokaryotes. However, it is now known that eukaryotic α- and β-tubulin are members of the conserved tubulin/FtsZ superfamily of assembling GTPases that perform essential cellular functions in not only eukaryotes, but prokaryotes as well (Lowe and Amos, 2009). In addition to α- and β-tubulin, the building blocks of MTs (Nogales et al., 1998), this family includes: the prokaryotic cell division protein FtsZ (Lowe and Amos, 1998), γ-

tubulin (Aldaz et al., 2005), bacterial tubulins BtubA/B (Schlieper et al., 2005), and the plasmid partitioning protein TubZ (Aylett et al., 2010; Ni et al., 2010). With the exception of γ-tubulin, which forms MT-nucleating ring complexes (γ-TuRC) (Kollman et al., 2010), all of the tubulin/FtsZ family members form polar filamentous structures with a GTP-binding site (Lowe and Amos, 2009). The filaments formed by this superfamily have variable properties and dynamics, all optimized for the specific functions they perform in their respective systems.

In eukaryotes, MTs are comprised of α- and β-tubulin monomers, which make up heterodimer subunits. Within the MT, these α/β-tubulin heterodimers organize into linear protofilaments that associate laterally to form a hollow, cylindrical tube. *In vivo*, the standard MT polymer contains 13 protofilaments and is 25nm in width, although variations on these parameters exist that give rise to MTs with special properties (Cueva et al., 2012; Desai and Mitchison, 1997). In cells, MT organizing centers (MTOCs) utilize γ-tubulin to provide a template for MT polymerization, speed up the rate of MT nucleation, and promote the formation of uniform MT polymers (Desai and Mitchison, 1997; Evans et al., 1985). *In vitro*, without the aid of MTOCs and accessory proteins, spontaneous MT nucleation is slower and the resulting MT polymers are non-uniform in width and protofilament number (Desai and Mitchison, 1997).

MTs are inherently polar structures; this polarity is essential for the function and dynamics of MTs and arises from the polar nature of the tubulin heterodimers that make

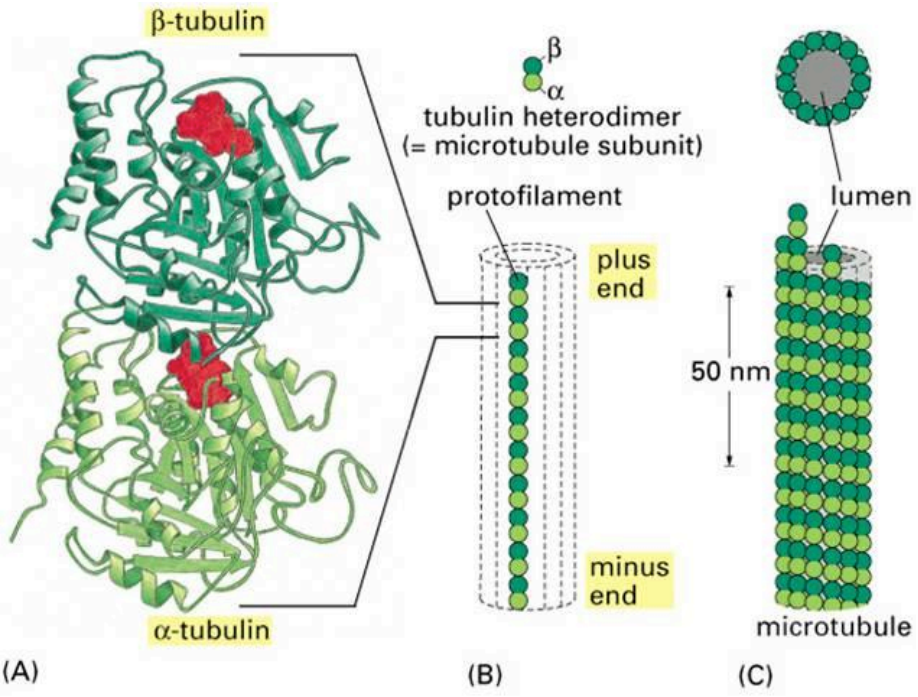

Figure 1: Microtubule structure.

Figure 1: Microtubule Structure.

(A) α- and β-tubulin structure in a tubulin heterodimer, the subunit of MTs. Light green=α-tubulin, dark green=β-tubulin, red=GTP-nucleotide. (B) Head-to-tail associations of tubulin heterodimers to form a linear protofilament. β-tubulin is oriented toward the plus-ends of MTs. (C) A 13 protofilament MT where lateral interactions between protofilaments are α to α and β to β except at the seam (not shown). Figure is adapted from *Molecular Biology of the Cell,* 4th Edition.

up the mature MT polymer. Each tubulin heterodimer binds two guanine nucleotides. Initially, during MT polymerization, both the α- and β-tubulin are bound to GTP; however, upon incorporation of heterodimers into the MT, the GTP bound to β-tubulin hydrolyses to GDP, while the GTP bound to α-tubulin is not hydrolyzed (Weisenberg and Deery, 1976). During polymerization, tubulin heterodimers self-orient in a head-to-tail manner (Amos and Klug, 1974): the GTP-bound α-tubulin is always oriented towards one end of the MT (the minus-end) and the GDP-bound β-tubulin (after hydrolysis) is always found at the opposing end (the plus-end) (Fan et al., 1996; Mitchison, 1993). This orientation provides polarity to the MT and creates two different ends of the polymer, each with their own dynamic properties.

MT dynamics are governed by dynamic instability. Dynamic instability can be described by four parameters: growth rate, shrinkage rate, frequency of switching from growth to shrinkage, and frequency of switching from shrinkage back to growth. Other related parameters can also be considered, such as the number of MT pauses and the frequency and duration of pause events. When a MT switches from growth to shrinkage, this is called catastrophe. On the other hand, when a MT switches from depolymerization back to growth, this is called a rescue. *In vitro*, both ends of MTs undergo phases of growth and shrinkage due to dynamic instability (Mitchison and Kirschner, 1984a, b); however, the plus-ends of MTs undergo rapid polymerization, while the minus-ends of MTs display slower dynamics (Allen and Borisy, 1974; Erickson and O'Brien, 1992; Walker et al., 1988). *In vivo*, dynamic instability is not readily

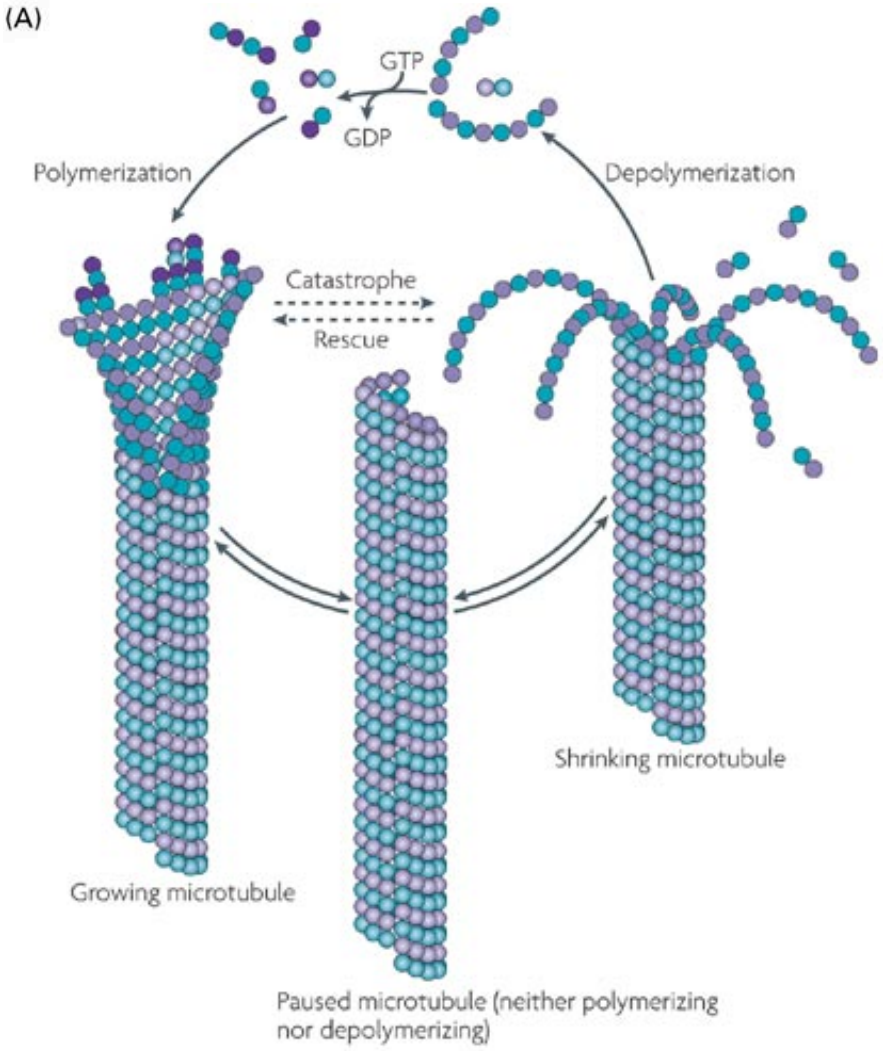

Figure 2: Microtubule dynamic instability.

Figure 2: Microtubule dynamic instability.

(A) Dynamic instability describes the coexistence of polymerizing and depolymerizing MTs. MTs frequently switch between phases of growth and shrinkages, with a switch from polymerization to depolymerization referred to as a catastrophe and a switch from depolymerization back to polymerization called a rescue. This dynamic nature of MTs is driven by GTP hydrolysis with loss of the stabilizing GTP cap at MT plus-ends leading to depolymerization events. Figure is adapted from *Conde and Caceres, 2009*.

observed at minus-ends of MTs because these ends are normally capped at MTOCs or undergo depolymerization when free in the cytoplasm (Desai and Mitchison, 1997). MT polarity is essential to many MT functions within the cell including, but not limited to, the creation of directional tracks within the cell, along which molecular motors walk for the transport of cellular cargos (Roberts et al., 2013; Vale and Fletterick, 1997).

GTP Hydrolysis and GTP Analogues

During MT polymerization, GTP-hydrolysis at the β-tubulin dimer occurs at a rate that is slower than polymerization itself (Carlier and Pantaloni, 1981). This results in the formation of a GTP-bound tubulin cap at the plus-ends of MTs and a MT lattice, which is comprised of GDP-bound tubulin (Mitchison and Kirschner, 1984a). As tubulin heterodimers undergo GTP-hydrolysis, a conformation change occurs, which has major implications on MT dynamics. GTP-bound tubulin exists in a straight conformation, while GDP-bound tubulin is more curved in nature; therefore, after hydrolysis occurs, tubulin in the MT polymer is under significant strain while forced to maintain a straight lattice structure (Desai and Mitchison, 1997; Melki et al., 1989). In this way, the energy of GTP hydrolysis is stored in the MT lattice as mechanical strain. The region of relatively straight GTP-tubulin at MT plus-ends, referred to as the GTP-cap, provides stability to the MT polymer by reinforcing the GDP-tubulin protofilaments in a straight conformation (Desai and Mitchison, 1997). Strain is released when GDP-tubulin subunits are exposed at MT plus-ends: this stored energy provides the driving force for the rapid depolymerization phase of dynamic instability. Loss of the stabilizing GTP-cap leads to

the curved protofilaments peeling away from the MT lattice during catastrophe (Tran et al., 1997) and, as these protofilaments disassemble, tubulin heterodimers are released back into the cytoplasm. Importantly, such dramatic changes in individual MT polymers allow for cellular remodeling of the MT network as a whole.

Although the conventional model is that GTP-tubulin is found at plus-ends of MTs and the MT lattice is comprised of GDP-tubulin, it was recently found that patches of GTP-tubulin also remain within the MT lattice after polymerization (Dimitrov et al., 2008). These patches, or GTP-tubulin remnants, may provide additional stability to the MT and are thought to allow for the binding of molecular motors to the lattice as well as the facilitation of rescue events (Dimitrov et al., 2008; Nakata et al., 2011). The discovery of GTP-tubulin remnants is an example of how complex and intricate the MT network is and hints that we still have a great deal to learn about this important branch of the cytoskeleton.

GTP hydrolysis provides an important basis of MT polarity as well as the energy for dynamic instability. Many analogues of GTP have been developed to aid in the study of MT properties and the behavior of MT binding proteins, especially *in vitro*. During GTP hydrolysis to GDP, the γ-phosphate bond in GTP is hydrolyzed to create GDP and P_i, or inorganic phosphate. Both inorganic phosphate and GDP are present within the MT lattice as an intermediate step during GTP hydrolysis. The inorganic phosphate is subsequently released, leaving behind GDP, and thereby completing the hydrolysis

cycle (Li and Kolomeisky, 2013). GTP analogues often have modifications in or near the γ-phosphate, which alter the GTP hydrolysis rate or capacity of GTP for hydrolysis.

One of the most widely utilized GTP analogues is GMPCPP (Guanosine-5'-[(α,β)-methyleno]-triphosphate). In GMPCPP, the P-O-P phosphoanhydride bond between the α- and β-phosphates is replaced with P-CH_2-P; despite the normal phosphoanhydride bond at the γ-phosphate, this modification is thought to result in incorrect geometry of GMPCPP when bound to β-tubulin (Hyman et al., 1992). The GMPCPP analogue undergoes negligible hydrolysis under standard conditions and, therefore, is considered to be a non-hydrolyzable mimetic of GTP (Hyman et al., 1992). Polymerization of GMPCPP-MTs occurs normally; however, their dynamic instability is suppressed (Desai and Mitchison, 1997). The use of this classic analogue has lead to many important findings regarding MTs, for example, that MT polymerization does not require GTP-hydrolysis itself and that tubulin bound to a GTP-like analogue provides stability to the MT lattice (Kirschner, 1978; Mejillano et al., 1990).

Another GTP analogue, GTPγS (Guanosine-5'-(γ-thio)-triphosphate), is a slowly hydrolyzable analogue that is thought to represent the GDP-P_i transition state, which occurs briefly between the hydrolysis of GTP to GDP. This transitional form of the guanine nucleotide is created during MT polymerization and is found at plus-ends of MTs. In GTPγS, an oxygen on the γ-phosphate of GTP is replaced with a sulfur atom; this sulfur substitution is thought to significantly hinder the release of inorganic

phosphate during hydrolysis and therefore mimic the GDP-P_i state. This analogue has been important in studies of MT plus-ends and the proteins that specifically localize there (Maurer et al., 2011; Maurer et al., 2012; Zanic et al., 2009).

Microtubule Associated Proteins (MAPs)

The cell has developed a vast assortment of proteins with the capacity to bind and regulate MTs, which are known as MT-associated proteins, or MAPs. Conventional MAPs, or structural MAPs, were the first subset of MAPs to be characterized; these proteins (MAP1, MAP2, tau, and MAP4) bind in a nucleotide-insensitive manner to the MT lattice and promote MT stability and assembly. This family of MAPs is essential for the structure and function of neurons and works to increase the percentage of tubulin present in the assembled polymer state (Desai and Mitchison, 1997).

MAPs regulate MTs and therefore must be tightly regulated themselves. One pervasive form of regulation is phosphorylation of MAPs. Phosphorylated forms of these proteins are generally inactive and have altered MT-binding properties. For example, phosphorylated tau can no longer stabilize MTs (Drechsel et al., 1992; Trinczek et al., 1995) or affect their dynamic properties (McNally, 1996).

Another important family of MAPs are the molecular motors that transport intracellular cargos and organelles along MTs. Motor proteins that move along MTs can be divided into two sub-families: kinesins and dynein, while myosins move along actin

filaments (Mallik and Gross, 2004). Dynein walks towards the minus ends of MTs (Mallik and Gross, 2004), while kinesins were conventionally considered to move towards the plus-ends of MTs (Hirokawa et al., 2009; Hirokawa et al., 1991). Further studies on the numerous kinesin families have shown that some kinesins have the capacity to walk towards the minus-ends of MTs and interestingly, can even interact with MTs in ways that do not involve transport of cargo (Desai and Mitchison, 1997; Hirokawa et al., 2009). Intriguingly, motors often appear to cooperatively, with intracellular transport of organelles employing multiple motors of different classes (Mallik and Gross, 2004). Motor proteins are highly regulated by multiple mechanisms including phosphorylation and autoinhibition (Verhey and Hammond, 2009).

MT Plus-End Tracking Proteins (+TIPs)

A unique group of MAPs, the MT plus-end tracking proteins (+TIPs), are nucleotide-sensitive and specifically localize to growing MT plus-ends (Akhmanova and Steinmetz, 2008; Schuyler and Pellman, 2001). Some +TIP proteins have the capacity to directly bind MT plus-ends, while others require binding to other proteins (hitchhiking) for their plus-end localization. The specific recruitment of +TIPs to plus-ends of MTs is thought to be due to their recognition of unique chemical and/or structural properties of the growing plus-end (Akhmanova and Steinmetz, 2008; Maurer et al., 2011; Maurer et al., 2012); however, a detailed molecular mechanism of this +TIP recognition is not fully understood.

Since the discovery of the first +TIP protein, cytoplasmic linker protein of 170 kDa (CLIP-170) (Diamantopoulos et al., 1999; Perez et al., 1999; Rickard and Kreis, 1990), several structurally and functionally diverse families of +TIP proteins have been characterized. +TIP proteins are evolutionarily conserved and are ideally positioned to play a role in the regulation of MT dynamics and many important MT based processes, such as cell division, cell migration, and trafficking of intracellular cargoes. The numerous +TIP proteins interact with each other at MT plus-ends to form a dynamic network of regulatory proteins that influence MT dynamics and function (Akhmanova and Steinmetz, 2008). The +TIP families most relevant to this study will be described in detail below.

End-binding Proteins (EBs)

End-binding proteins (EBs) are a highly conserved and ubiquitous family of +TIP proteins. In mammalian cells, there are three EB family members (EB1, EB2, and EB3), which differentially track MTs: EB1 and EB3 form distinct comet like structures at MT plus-ends, while EB2 is more dispersed along the MT lattice displaying only a slight accumulation at the tip (Komarova et al., 2009). EBs are unique because they are one of the few +TIP families that can autonomously track MT plus-ends *in vitro* ((Bieling et al., 2007) and others). They are considered the master regulators of the +TIP network because most +TIPs do not directly bind MT plus-ends, but rely on interactions with EBs for their plus-end localization (Akhmanova and Steinmetz, 2008; Komarova et al., 2009). As major regulators of +TIP network composition, as well as through their direct

influence on MT dynamics, EBs to a large extent control all types of MT-dependent processes.

Autonomous localization of EBs to MT plus-ends indicates that they directly recognize a distinct, but transient feature at MT tips. EBs display high affinity for MT plus-ends compared to the MT lattice and it has been proposed that EBs can sense the nucleotide state of a MT (Maurer et al., 2012; Zanic et al., 2009). Specifically, it has been shown *in vitro* that EBs have low affinity for GDP-tubulin, high affinity for GTP-tubulin, and even greater affinity for GDP-P_i-tubulin (represented by GTPγS-MTs) (Maurer et al., 2011; Zanic et al., 2009). It is not yet clear whether EBs recognize the nucleotide state itself, a nucleotide-dependent conformational change in tubulin, or a combination of these features.

Analyses of the EB family members have shown that almost the entire EB surface is conserved, which indicates that EBs undergo significant protein-protein interactions (Buey et al., 2011). This high level of conservation is consistent with the role of EBs as the +TIP complex master regulators (Lansbergen and Akhmanova, 2006; Tirnauer and Bierer, 2000). The conserved Calponin homology (CH) domain at the N-terminus of EBs mediates their MT binding (Hayashi & Ikura 2003), while multiple EB functions are attributed to their C-terminal domains, which allow EB dimerization (coiled coil and EB homology domain) as well as recruitment of other +TIP proteins to the plus-ends of MTs (EB homology domain and EEY/F motif) (Akhmanova & Steinmetz 2008).

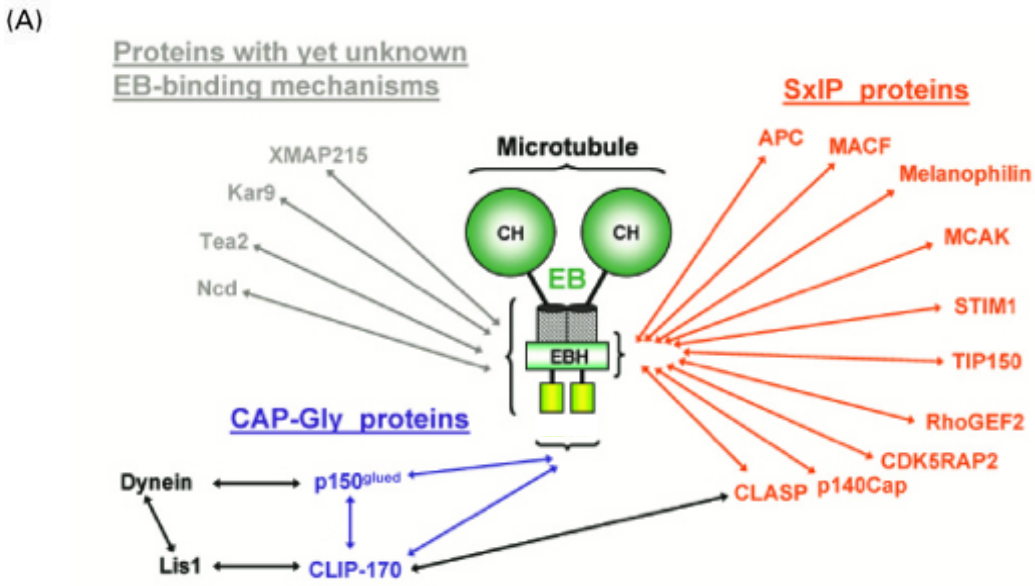

Figure 3: End-binding proteins: Master organizers of the +TIP complex.

Figure 3: End-binding proteins: Master organizers of the +TIP complex.

(A) Depiction of the various +TIP families that require binding to EBs for plus-end localization. Orange=SxIP proteins (including CLASPs), blue=CAP-Gly proteins, grey=proteins with unknown EB-binding mechanisms or proteins that tip track in an EB-independent manner. SxIP proteins associate with EBs via interactions with the EB homology (EBH) domain, while CAP-Gly proteins bind the EEY/F motif (not shown) at the C-terminal tail of EBs. Figure is adapted from www.psi.ch/lbr/steinmetz-group-research.

A hydrophobic cleft in the EB homology domain mediates binding of SxIP-containing proteins to EBs (Honnappa et al., 2009); due to the large number of +TIP proteins containing SxIP motifs, the SxIP sequence is considered to be a widespread MT plus-end localization signal (Buey et al., 2012; Honnappa et al., 2009). Interestingly, an EEY/F motif is positioned at the very C-terminal end of EBs, which mimics the E-hook of tubulin (Akhmanova & Steinmetz 2008) and mediates interactions of EBs with the CAP-Gly (Cytoskeleton-associated protein with a conserved Glycine) domain-containing family of +TIP proteins (Komarova et al., 2005; Weisbrich et al., 2007). Currently, little is known about regulation of mammalian EBs and how their interactions with MTs may be influenced by other +TIPs.

CLIP-Associated Proteins (CLASPs)

CLIP-Associated Proteins (CLASPs) were first isolated as a result of their capacity to bind an already isolated +TIP, CLIP-170 (Akhmanova et al., 2001). It is now known that CLASPs are an important class of +TIP proteins and components of the +TIP complex at MT tips. CLASPs are conserved over evolution and, in mammalian cells, there are two largely redundant proteins, CLASP1 and CLASP2 (Akhmanova et al., 2001). Additionally, each CLASP protein has multiple isoforms that display cell-type specific expression levels and that carry out specific functions in the cell (Akhmanova et al., 2001; Mimori-Kiyosue et al., 2005). CLASPs regulate MT dynamics and interact directly with MTs and a number of +TIP proteins, including EBs (Akhmanova and Steinmetz, 2008).

CLASPs are unique members in the +TIP family because they display biased MT-binding behavior based on their location in the cell: in the cell body, CLASPs exhibit classic +TIP behavior and support persistent MT growth by binding MT plus-ends and promoting MT rescues (Mimori-Kiyosue et al., 2005). In addition, CLASPs can stabilize MTs at the leading edge of migrating cells by binding along the lattice of pioneer MTs (Akhmanova et al., 2001; Wittmann and Waterman-Storer, 2005). Recently, the fission yeast homolog of CLASPs has been shown to bind free tubulin dimers and promote their incorporation into the MT lattice. This activity of CLASP is thought to be a major factor in the mechanism behind the promotion of rescue events by CLASPs (Al-Bassam et al., 2010).

The diverse functions of CLASPs at MTs are attributed to their Tumor Overexpressed Gene (TOG) domains. CLASP proteins share this conserved TOG domain with the XMAP215/Dis1 family; proteins in this family have anywhere from two to five TOG domains, which often vary in their organization (Al-Bassam and Chang, 2011). Interestingly, CLASP proteins contain conventional TOG domains as well as cryptic-TOG or TOG-like domains, which lack clear TOG domain sequence homology. These TOG-like domains were initially considered to be divergent from the conventional TOG domains in the XMAP215/Dis1 family (Slep, 2009) despite their implication in MT binding and regulation (Al-Bassam et al., 2010; Patel et al., 2012); Recent investigations have revealed that the CLASP TOG-like domains are in fact true TOG domains, but with a unique bent architecture (Leano et al., 2013). Accordingly, it has been proposed that

the distinctive bend in CLASP TOG domains may explain the unique MT regulatory properties of CLASPs that distinguish them from the other members of the XMAP215/Dis1 family (Wilbur and Heald, 2013).

Interactions Between EBs and CLASPs

In addition to their association with the MT lattice, CLASPs rely on interactions with EBs to efficiently localize to MT plus-ends (Mimori-Kiyosue et al., 2005). CLASPs contain a basic EB-binding domain, which includes two SxIP motifs (Patel et al., 2012). As previously mentioned, SxIP motifs mediate protein binding to the hydrophobic cavity of EBs near their C-terminal tail (Buey et al., 2012). It is important to note that, in fission yeast, although CLASP associates with EB1, its stabilizing affect on MTs is independent of other +TIPs suggesting that CLASPs directly regulate MTs (Bratman and Chang, 2007).

The interaction of CLASPs and EBs is highly regulated via phosphorylation and determines which of CLASP's MT localization patterns will prevail in a given area of the cell: the degree of CLASP phosphorylation mediates a switch between EB binding and MT lattice association (Kumar et al., 2012; Kumar et al., 2009; Wittmann and Waterman-Storer, 2005). Multiple kinases have been implicated in the regulation of this localization switch, with GSK3 acting as a major player (Akhmanova et al., 2001). Local GSK3 inactivation (Etienne-Manneville and Hall, 2003) by Rac at the leading edge of migrating cells results in CLASP dephosphorylation and coating of the lattice to promote

MT stability in this region (Wittmann and Waterman-Storer, 2005). In the cell body, low levels of CLASP phosphorylation by GSK3 impede the electrostatic interactions required for MT lattice binding, while promoting CLASP-EB interactions leading to CLASP plus-end recruitment by EBs (Kumar et al., 2009). Extensive multisite phosphorylation in this MT/EB-binding region abolishes CLASP interactions with both the MT lattice and EBs (Kumar et al., 2012; Kumar et al., 2009; Wittmann and Waterman-Storer, 2005). The region of CLASP1 and CLASP2 that undergoes phosphorylation is nearly identical and highly conserved indicating that their localization patterns are regulated in the same manner (Kumar et al., 2012). Interestingly, in a similar manner to CLASP at the cell periphery, CLASPs perform a unique function at the Golgi complex where they stabilize newly nucleated Golgi-derived MTs (Efimov et al., 2007; Miller et al., 2009).

In cells, close examination of CLASP and EB localization reveals that these proteins colocalize at MT plus-ends, but that CLASP localization lags slightly behind EB comets ((Mimori-Kiyosue et al., 2005) and our unpublished results). This localization suggests that, although, in mammalian cells, CLASPs depend on EBs for their plus-end recruitment, CLASPs also function separately from EBs at MT tips. Importantly, the capacity of CLASPs to independently bind the lattice of MTs also suggests that CLASP may influence MT lattices directly. These unique properties of CLASPs make them ideal candidates for the regulation of EBs at MTs.

Thesis Summary

The work presented in this thesis summarizes years of scientific investigation on the properties and functions of the MT network and the diverse proteins that bind and regulate MTs. Specifically, this work highlights the exciting new field of +TIP proteins and their master regulators, the EB proteins. An emphasis in the field has been on elucidating the role of EBs in the control of the +TIP network; however, it is yet to be determined how other +TIP proteins influence EB localization and interactions at MTs.

In Chapter II, I report my findings that CLASPs are crucial determinants of proper EB localization at MTs in mammalian cells. This chapter starts with the initial observation that, in CLASP-depleted cells, EB1 and EB3 relocalize to the MT lattice in addition to their characteristic plus-end localization. This striking alteration in EB localization is the first example of another +TIP family regulating EB localization at MTs. Further studies lead to the illumination of a possible mechanism for CLASP-dependent EB localization, in which CLASP promotes GTP hydrolysis at the MT lattice to reduce high affinity EB binding sites at this location and, as a result, restrict EB binding to the plus-ends of MTs.

Chapter III highlights the important contributions of this work to the +TIP field as well as several possible directions this project could take in the future. Although this thesis establishes CLASPs as important regulators of EBs, and potentially of the whole

+TIP network, there is still much work to be done before the regulation and functions of this dynamic network can be fully understood.

CHAPTER II

CLASPs ARE REQUIRED FOR PROPER MICROTUBULE LOCALIZATION OF END-BINDING PROTEINS

Abstract

Microtubule (MT) plus-end tracking proteins (+TIPs) preferentially localize to MT plus-ends. End-binding proteins (EBs) are master regulators of the +TIP complex; however, it is unknown whether EBs are regulated by other +TIPs. Here, we show that Cytoplasmic linker associated proteins (CLASPs) modulate EB localization at MTs. Strikingly, in CLASP-depleted cells, EBs localized along the MT lattice in addition to plus-ends. The MT-binding region of CLASP was sufficient for restoring normal EB localization, while neither EB-CLASP interactions nor EB tail-binding proteins are involved. *In vitro* assays revealed that CLASP directly functions to remove EB from MTs. Importantly, this effect occurs specifically during MT polymerization, but not at pre-formed MTs. Increased GTP-tubulin content within MTs in CLASP-depleted cells suggests that CLASP facilitates GTP-hydrolysis to reduce EB lattice binding. Together, these findings suggest that CLASPs influence the MT lattice itself to regulate EB and determine exclusive plus-end localization of EBs in cells.

Introduction

MTs are inherently polar structures polymerized from GTP-bound tubulin heterodimers, which incorporate at the growing MT plus-end. The slower rate of GTP hydrolysis, compared to that of MT polymerization, results in a stabilizing GTP-tubulin cap at the plus-ends of MTs (reviewed in (Desai and Mitchison, 1997). +TIPs are a diverse group of evolutionarily conserved MT-associated proteins (MAPs) that specifically localize to the dynamic plus-end of MTs (Schuyler and Pellman, 2001). +TIPs are ideally positioned to regulate MT dynamics and play an important role in many MT-based processes. Within the +TIP family, EBs are notable in their ability to autonomously recognize a transient feature at growing MT plus-ends with great specificity (Bieling et al., 2007). In mammalian cells, there are three EB family members: EB1, EB2, and EB3. EB1 and EB3 are well studied and are similar in their structure, localization, and behavior, while EB2 is more divergent in structure and has not been extensively studied (Buey et al., 2011; Komarova et al., 2009). Recent work has revealed that EBs localize to MT tips due to their ability to sense the nucleotide-state as well as the specific conformation of tubulin at MT plus-ends (Maurer et al., 2011; Maurer et al., 2012; Zanic et al., 2009). The majority of +TIPs require binding to the EB tail region, via various localization signals (SxIP (Honnappa et al., 2009) or CAP-Gly (Weisbrich et al., 2007)), to achieve their specific comet-like localization (reviewed in (Akhmanova and Steinmetz, 2008)); for this reason, EBs are considered the master regulators of the +TIP network.

Within this network, CLASPs are a unique class of +TIPs that exhibit two specific MT localizations. On one hand, CLASPs support persistent MT growth by binding MT plus-ends and promoting MT rescues (Akhmanova et al., 2001; Mimori-Kiyosue et al., 2005); on the other hand, CLASPs can stabilize specialized MT subsets by binding along the MT lattice, for example pioneer MTs at the leading edge of migrating cells (Wittmann and Waterman-Storer, 2005) or newly nucleated Golgi-derived MTs (Efimov et al., 2007; Miller et al., 2009). In mammalian cells, there are two CLASP family members, CLASP1 and CLASP2, which play partially redundant roles and rely on interactions with EBs (via the basic/SxIP region) to localize to MT plus-ends (Mimori-Kiyosue et al., 2005). In fission yeast, although CLASP associates with EB1, its stabilizing affect on MTs is independent of other +TIPs suggesting that CLASP directly regulates MTs (Bratman and Chang, 2007). Of note, CLASPs also independently bind tubulin heterodimers and associate with the MT lattice through their TOG (tumor overexpressed gene) domains (Al-Bassam et al., 2010; Al-Bassam et al., 2007). Here, we report evidence that CLASPs are crucial determinants of proper EB localization at MTs in mammalian cells.

Results

EB proteins localize to the MT lattice in CLASP-depleted cells

Although it is well established that EBs are the master regulators of the +TIP network, it is unknown whether other +TIPs regulate EB localization at MTs. Strikingly, we found that, upon depletion of CLASP1 and CLASP2 (herein referred to as CLASPs), endogenous EB1 (Figure S1A-B) and EB3 (Figure 1A-B) both bind along the MT lattice in addition to their characteristic plus-end localizations. This dramatic change in EB localization is quantified by line scan analysis of EB fluorescence intensity along a MT (Figure 1H). CLASP-dependent EB redistribution was observed in multiple cell types; rat vascular smooth muscle cells A7r5 (Fig. 1A-B, S1A-B), human retinal pigment epithelial cells RPE1 (Fig. 2A-B), mouse embryonic fibroblasts (MEF), African green monkey kidney fibroblasts (COS-7), and cancer cells of human and mouse origin HeLa, B16-F1 and Caco-2 (Figure S2) are shown in this study. CLASP-dependent EB localization is therefore not cell type specific. Because EB2 always exhibits significant MT lattice localization (Komarova et al., 2009), and its positioning was not changed upon CLASP depletion (not shown), we focused our studies on the EB1 and EB3 proteins (herein referred to as EBs). Interestingly, depletion of CLASP1 or CLASP2 individually (Figure S1J) resulted in partial redistribution of endogenous EB1 and EB3 along the MT lattice of A7r5 cells indicating that both CLASPs have the capacity to regulate EBs (Figure S1D-I); a combination of siRNAs against both CLASPs was used for all subsequent CLASP-depletion experiments (Figure 1E) and non-targeting (NT) siRNA was used as a control.

As overexpression of EBs results in lattice decoration, we first confirmed that endogenous levels of EB1 protein did not increase upon CLASP-depletion (Figure 1F,I). Because CLASPs promote MT stability, CLASP-depletion leads to MT destabilization, altered MT dynamics, and a sparse MT network (Akhmanova et al., 2001; Mimori-Kiyosue et al., 2005). Therefore, it is in principle possible that an increased EB to MT ratio causes the enhanced EB lattice binding observed in CLASP-depleted cells. However, in cells briefly treated with the MT depolymerizing drug Nocodazole to decrease MT numbers (Figure 1C,N), no significant relocalization of EB3 to the MT lattice was observed (Figure 1C). As an additional control, GFP-Stathmin, which sequesters free tubulin dimers, was expressed for 72 hours (the same time as CLASP siRNA treatment); GFP-Stathmin expressing cells also had decreased MT numbers (Figure 1D,N), but did not show a significant increase in EB3 lattice binding (Figure 1D,H). Total MT length did not significantly differ between the CLASP-depleted, Nocodazole-treated and GFP-Stathmin-expressing cells (Figure 1N) indicating that these controls effectively mimic the reduced MT number observed in CLASP-depleted cells. Moreover, the number of EB plus-ends upon CLASP-depletion and GFP-Stathmin expression did not statistically differ (Figure S2L). Importantly, in both Nocodazole treatment and GFP-Stathmin expression, EB1 protein levels were not statistically different from NT control (Figure 1G,J and Figure S1K).

To further confirm that EB lattice binding in CLASP-depleted cells is not an artifact of an increased EB to MT ratio, we performed a partial depletion of EB1, either

alone or in addition to CLASP-depletion (Figures 1M and S1M) and then performed line scan analysis to quantify the ratio of EB1 bound to the lattice vs. the tip of MTs (Figure 1K). In the single depletion of CLASPs, our line scans showed a lattice to tip ratio of 0.48 ± 0.03; similarly, upon double depletion of EB1 and CLASPs together, the lattice to tip ratio was 0.41 ± 0.03 (Figure 1L). This difference was not statistically significant indicating that, regardless of the amount of EB protein in the cell, CLASP-depletion has the same affect of increased EB lattice binding. Thus, the altered EB localization in cells lacking CLASPs cannot be explained by an increased EB to MT ratio.

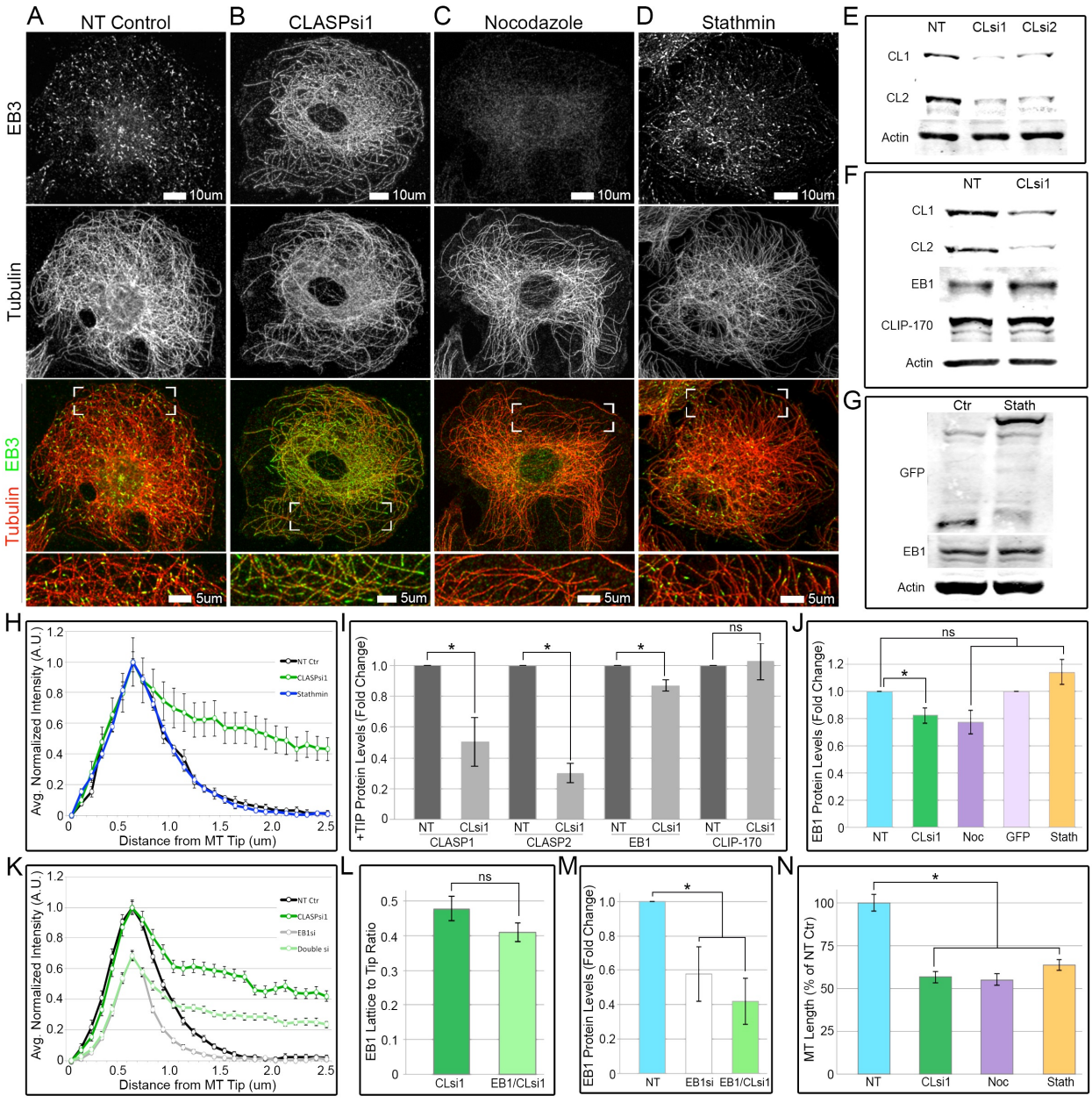

Figure 1: Localization of EB proteins at microtubules is altered in CLASP-depleted cells.

Figure 1: Localization of EB proteins at microtubules is altered in CLASP-depleted cells.

(A-D) Immunofluorescence images of A7r5 cells stained for α-tubulin (red) and EB3 (green). (A) EB3 localizes to MT plus-ends in NT control cells. (B) EB3 extensively coats the MT lattice, in addition to its normal plus-end localization, in CLASP-depleted cells (CLASPsi1). (C) EB3 does not significantly localize to the MT lattice in Nocodazole treated cells. (D) EB3 localizes to MT plus-ends and does not significantly localize to the MT lattice in GFP-Stathmin expressing cells. (A-D) Merge zoomed region is indicated by boxed corners in Merge. White box indicates scale bar. (E) Western blot of A7r5 whole cell lysate showing significant reduction in both CLASP1 and CLASP2 protein levels, using two different combinations of siRNAs, when compared to NT control. (F) Western blot of HeLa whole cell lysate showing no change in EB1 and CLIP-170 protein levels upon CLASP-depletion when compared to NT control. (G) Western blot of A7r5 whole cell lysate showing no change in EB1 protein levels upon GFP-Stathmin expression when compared to GFP-control. (E-G) Actin was used as a loading control. (H) Line scans showing distribution of EB3 at MTs in NT control (black), CLASP-depletion (green), or GFP-Stathmin expression (blue). Based on data similar to (A,B,D). (I) +TIP levels by western blot analysis in NT control and CLASP-depletion. (J) EB1 levels by western blot analysis in NT control, CLASP-depletion, Nocodazole treatment, and GFP-control or GFP-Stathmin expression. (K) Line scans showing distribution of EB1 at MTs in NT control (black), CLASP-depletion (green), EB1 partial depletion (grey), or

EB1/CLASP double depletion (light green). (L) Quantification of EB1 lattice to tip ratio in CLASP-depletion and EB1/CLASP double depletion based on line scan analysis in (K). (M) EB1 levels by western blot analysis in NT control, EB1 partial depletion, and EB1/CLASP double depletion. (N) Average total MT length in NT control, CLASP-depletion, Nocodazole treatment, and GFP-Stathmin expression. Based on data similar to (A-D). (H,K,L) Line Scan and lattice to tip ratio values are normalized mean intensities ± S.E.M. (n=50, 2 independent experiments). (I,J,M) Graphs are normalized means ± S.E.M in 3 independent experiments. (H-N) Student's unpaired two-tailed t-test. Asterisks, $p<0.05$. (A-N) CLASPsi1/CLsi1=siRNA combination 1. CLsi2=siRNA combination 2. See also Figures S1 and S2.

+TIP proteins relocalize with EBs in CLASP-depleted cells

We next sought to determine whether CLASP influenced the localization of other +TIP families at MTs, or if CLASP regulation of EB localization was specific. We screened CLASP-depleted cells for localization of representative proteins from the major +TIP families: CAP-Gly proteins, SxIP proteins, and chTOG, which localizes to MT plus-ends in an EB-independent manner (Brouhard et al., 2008). The CAP-Gly proteins, CLIP-170 and $p150^{Glued}$, relocalized to the MT lattice upon CLASP-depletion and their localization was indistinguishable from lattice-bound EB1 and EB3 respectively (Figures 2 and S3A-B). The endogenous protein expression levels of CLIP-170 did not change upon depletion of CLASPs (Figure 1F,I). Expression of the SxIP proteins, GFP-SLAIN2 (Figure S3C-D) and a minimal EB-Binding Domain of Dystonin (GFP-Dst-EBBD, Figure S3E-F) relocalized to the MT lattice upon CLASP-depletion in a similar manner; the localization of this minimal construct requires EB-binding and is independent of other interacting partners. Interestingly, another SxIP protein, APC, did not change its characteristic localization to peripheral patches, as well as to occasional MT plus-ends, upon CLASP-depletion (Figure S3G-H). A possible explanation for this behavior is that APC interacts with a large number of other proteins in the cell and it is unclear to what extent APC's interaction with EBs is essential for its localization pattern (Kita et al., 2006). Similarly, chTOG did not relocalize to the MT lattice upon CLASP-depletion (Figure S3I-J). A lack of chTOG binding to the MT lattice is likely explained by the ability of chTOG to track MT plus-ends independently of EBs.

To examine whether CLASPs directly regulate CAP-Gly and SxIP protein localization at MTs, or if these proteins simply follow EB to the MT lattice, we took advantage of a previously described approach. It has been shown that the GFP tag on the C-Terminus of EB3 occludes binding of CLIP-170 to the EEY/F tail of EB3; therefore, expression of EB3-GFP in cells displaces CLIP-170 from MT plus-ends by a dominant negative mechanism (Lomakin et al., 2009; Skube et al., 2010). We observed that EB3-GFP, similar to endogenous protein, relocalizes to the MT lattice in CLASP-depleted cells (Figure 2F,K). Interestingly, upon CLASP-depletion in cells expressing EB3-GFP, CLIP-170 did not relocalize to the MT lattice, in contrast to un-transfected cells lacking CLASP (Figure 2D,F,K). We have further designed an Emerald-EB3 construct, which allows for proper EB localization to MTs as well as correct localization of CLIP-170 to MT plus-ends (Figure 2G) indicating that this construct indeed allows for normal CLIP-170 interactions with EBs. In CLASP-depleted cells, both Emerald-EB3 and CLIP-170 significantly relocalize to the MT lattice (Figure 2H,L), resembling un-transfected CLASP-depleted cells (Figure 2D). These experiments reveal that CLIP-170 binding to the MT lattice in CLASP-depleted cells is indeed dependent upon CLIP-170 interaction with the C-terminus of EBs. Together with relocalization of the Dystonin minimal EB-binding domain, these data suggest that, upon CLASP-depletion, both CAP-Gly and SxIP proteins likely follow EBs to the lattice rather than being independently regulated by CLASPs.

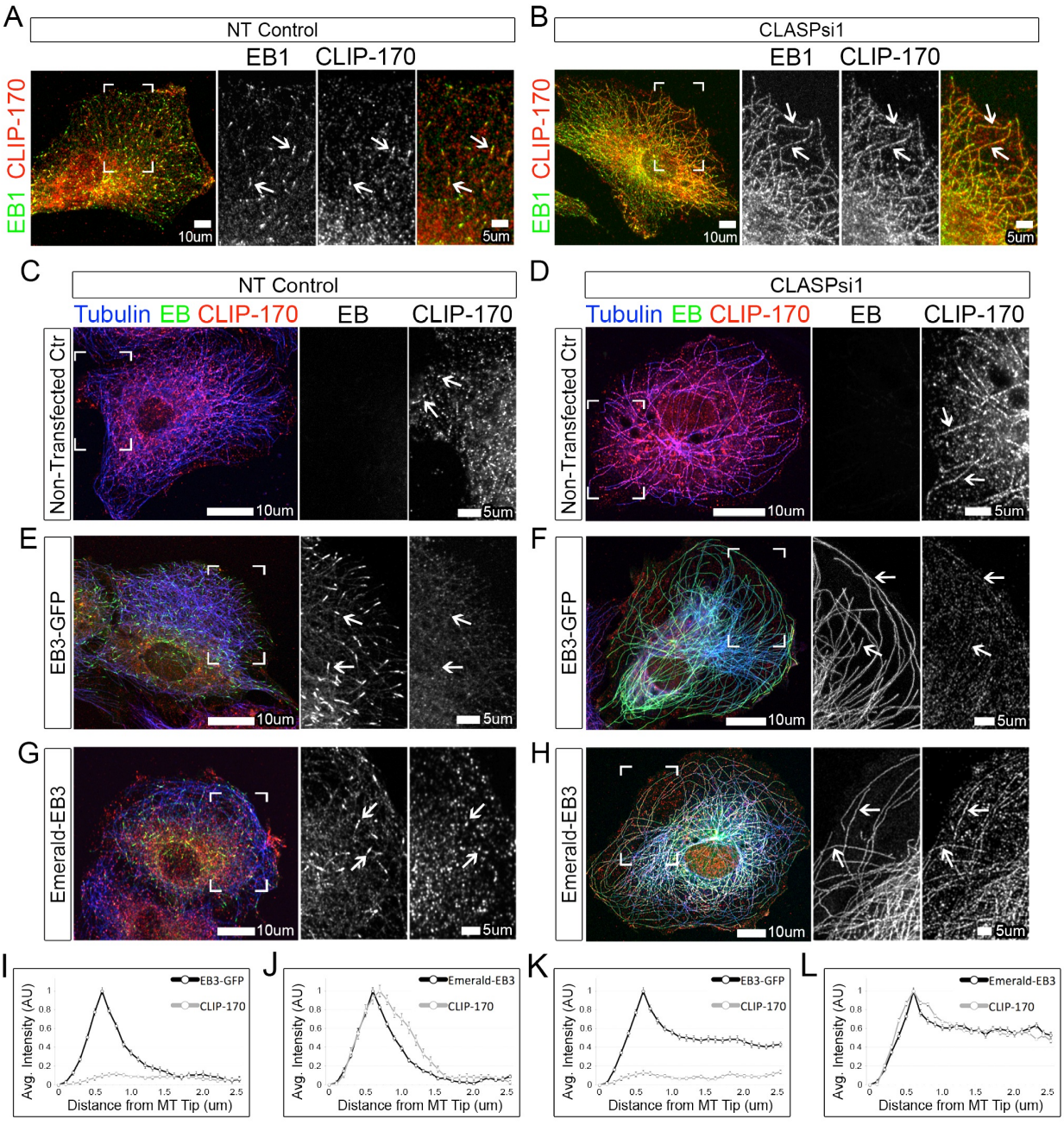

Figure 2: CAP-Gly proteins follow EBs to the microtubule lattice in CLASP-depleted cells.

Figure 2: CAP-Gly proteins follow EBs to the microtubule lattice in CLASP-depleted cells.

(A-B) RPE cells stained for EB1 (green) and CLIP-170 (red). (A) EB1 and CLIP-170 both localize to MT plus-ends in NT control cells. (B) In addition to EB1, CLIP-170 also relocalizes to the MT lattice in CLASP-depleted cells. (C-H) A7r5 cells expressing exogenous EB3 (green), and stained for CLIP-170 (red) and α-tubulin (blue, pseudo-colored). (C) CLIP-170 localizes to MT plus-ends in un-transfected NT control cells, (D) CLIP-170 coats the MT lattice in CLASP-depleted cells. (E) In NT control cells expressing EB3-GFP, EB3-GFP localizes to MT plus-ends, while CLIP-170 localization to plus-ends is greatly reduced. (F) In CLASP-depleted cells expressing EB3-GFP, EB3-GFP relocalizes to the MT lattice, while lattice-bound CLIP-170 is significantly reduced. (G) In NT control cells expressing Emerald-EB3, both Emerald-EB3 and CLIP-170 localize to MT plus-ends. (H) In CLASP-depleted cells expressing Emerald-EB3, both Emerald-EB3 and CLIP-170 coat the MT lattice. (A-H) Merge zoomed region is indicated by boxed corners in Merge. White box indicates scale bar. (C-H) White arrows show examples of EB/CLIP-170 characteristic localization, CLIP-170 displacement, or EB/CLIP-170 lattice relocalization respectively. (I-L) Line scans showing distribution of CLIP-170 (grey) at MTs in cells expressing either EB3-GFP or Emerald-EB3 (black). Based on data similar to (E-H). (A-H) Immunofluorescence. Values are normalized mean intensities ± S.E.M. (n=50, 2 independent experiments). Student's unpaired two-tailed t-test. CLASPsi1=siRNA combination 1. See also Figure S3.

TOG2 region of CLASP, but not EB binding, is required to restore normal EB plus-end localization

To gain insight into the mechanism of CLASP-dependent regulation of EB localization at MTs, we determined which domains of CLASP are required for the exclusive plus-end localization of EBs. For these experiments, we utilized various CLASP mutant constructs (Figure 3, individual cellular localizations shown in Figure S4) and tested for their capacity to rescue EB localization in CLASP-depleted cells. Previous studies have outlined three main protein-interacting regions in CLASP: The TOG and TOG-like domains confer MT binding (Al-Bassam et al., 2007; Patel et al., 2012), while the basic/SxIP region allows for EB binding (Mimori-Kiyosue et al., 2005; Patel et al., 2012), and the C-terminus mediates CLASP dimerization as well as interactions with multiple protein partners such as CLIP-170 (Akhmanova et al., 2001), GCC185 (Efimov et al., 2007), and LL5β (Lansbergen et al., 2006). Recent findings have revealed that the TOG-like domains, or cryptic TOG domains, of CLASPs are in fact true TOG domains, but with a unique bent architecture (CLASP1 TOG-like 1: (Leano et al., 2013); and CLASP2 TOG-like 2: our unpublished results). For this study, the first TOG-like domain (TOG-like 1) will be referred to as the TOG2 domain and the last TOG-like domain (TOG-like 2) will be referred to as the TOG3 domain. As expected, re-expression of full-length wild-type CLASP2 in CLASP-depleted cells rescued characteristic plus-end localization of endogenous EB3 in A7r5 cells (Figure 3D).

Intriguingly, CLASP constructs with mutated SxIP motifs readily rescued EB plus-end localization (Figure 3E); because the SxIP motif is essential for CLASP binding to EBs, this result indicates that CLASPs-EB interactions are not involved in the observed phenomenon. To confirm this conclusion, we utilized an artificial dimer of the EB3 CH MT-binding domain (EB3-N-LZ-GFP, previously described in (Komarova et al., 2009)), which lacks the tail region of EB, or the EB cargo region, that allows for interactions with CLASPs as well as other +TIP network proteins. We found that exogenously expressed EB3-N-LZ-GFP, which is normally confined to MT plus ends (Figure 3Q and (Komarova et al., 2009)), clearly localized along the MT lattice in CLASP-depleted cells (Figure 3R). This result indicates that: 1) CLASP-EB interactions are not necessary for CLASP to influence EB localization at MTs, 2) binding of other EB-interacting proteins to EB is not required for this regulation, and 3) EB lattice redistribution cannot be due the recruitment of EB to the lattice by another EB tail-binding MAP when CLASPs are not present. Together, these data support a model in which CLASPs alter the MT itself to restrict EB-MT interactions to the MT tip (Figure 4J) and indicates that EB tail-binding proteins are not involved in this response.

Further rescue experiments with CLASP mutant constructs revealed that the TOG3 domain of CLASP, which mediates weak MT binding, was also dispensable for regulating EB localization (Figure 3F), while the TOG2 domain was required (Figures 3G and 3H). Importantly, the TOG2 domain of CLASP has been reported to mediate strong interactions between CLASP and MTs (Patel et al., 2012).

To test whether the TOG2 domain of CLASP was sufficient to rescue EB localization in CLASP-depleted cells, we re-expressed the truncated monomeric TOG2 domain. Monomeric TOG2 alone was not sufficient to restore EB plus-end localization (Figure 3L), but truncated CLASP mutants containing both the TOG2 and TOG3 domains did rescue (Figures 3I and 3J), suggesting that TOG2 plus an additional weak MT-interacting region may be sufficient for CLASP-dependent regulation of EBs. In fact, monomeric TOG2 linked to the Ensconsin MT-binding domain (EMTB), or TOG2 directly linked to the C-terminus of CLASP (TOG2-C), were both able to rescue EB plus-end localization. Addition of the C-terminal domain of CLASP likely promotes MT-binding of the TOG2-C construct via TOG2 dimerization (Al-Bassam et al., 2010; Patel et al., 2012); however, it cannot be ruled out that the C-terminus itself weakly interacts with MTs, which has been previously proposed (Wittmann and Waterman-Storer, 2005). Nevertheless, the C-terminal domain of CLASP was not strictly required to rescue EB localization (Figure 3I), which reveals that CLASP does not need to bind its cellular partners for the regulation of EB distribution along MTs. Together, these CLASP mutant studies demonstrate that the N-terminal MT-binding region of CLASP (TOG2 domain) combined with an additional weak MT interaction (e.g. TOG3 or C-terminus of CLASP), is necessary and sufficient to restore characteristic EB localization. Accordingly, we suggest that CLASP influences the MT lattice itself to promote normal EB plus-end distribution.

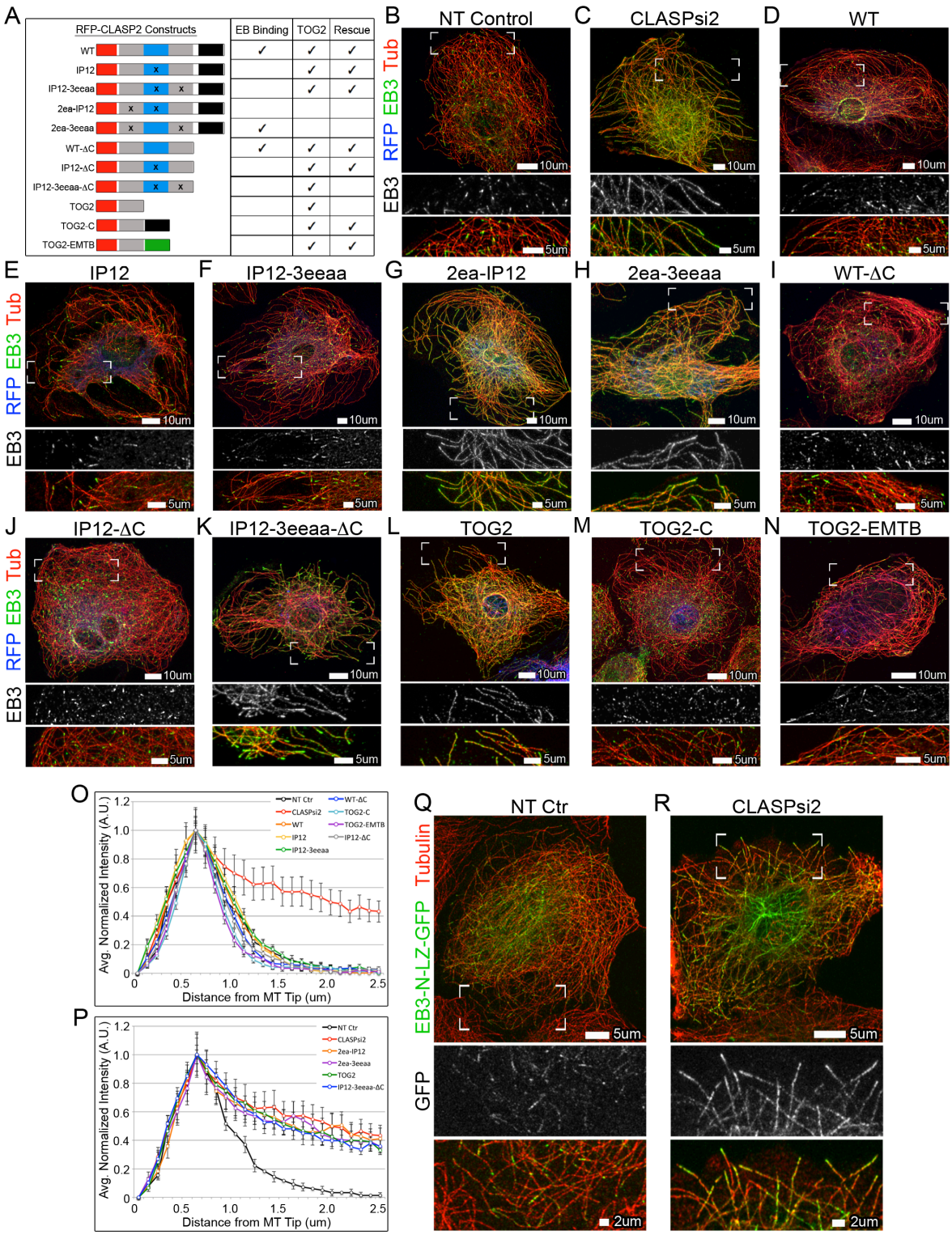

Figure 3: TOG2 domain of CLASP is necessary to restore normal EB plus-end localization.

Figure 3: TOG2 domain of CLASP is necessary to restore normal EB plus-end localization.

(A) Schematic representation of RFP tagged WT-CLASP2 as well as mutant CLASP2 rescue constructs. Red=RFP tag, grey=TOG-containing MT binding domains (TOG2 and TOG3), blue=EB-binding region (basic/SxIP), black=C-Terminus, and green=MT-binding domain of Ensconsin (EMTB). Capacity for each construct to bind EB and rescue normal EB tip localization is shown. (B) EB3 localizes to MT plus-ends in NT control cells. (C) EB3 extensively coats the MT lattice, in addition to its normal plus-end localization, in CLASP-depleted cells. (D-N) A7r5 cells expressing various RFP-CLASP2 rescue constructs (pseudo-colored blue) stained for endogenous EB3 (green) and α-tubulin (pseudo-colored red). (D,E,F,I,J,M,N) CLASP-depleted cells expressing WT (D), IP12 (E), IP12-3eeaa (F), WT-ΔC (I), IP12-ΔC (J), TOG2-C (M), or TOG2-EMTB (N) rescue constructs all restore normal EB3 plus-end localization. (G,H,K,L) CLASP-depleted cells expressing 2ea-IP12 (G), 2ea-3eeaa (H), IP12-3eeaa-ΔC (K), or TOG2 (L) rescue constructs were not sufficient to restore normal EB3 plus-end localization and EB3 can be seen along the MT lattice. (O-P) Line scan analysis quantifying rescue of normal EB3 plus-end localization by expression of rescue constructs in CLASP-depleted cells (O) or cells expressing constructs unable to rescue EB3 location in CLASP-depleted cells (P). (O-P) Line scan values are normalized mean intensities ± S.E.M. (n=50, 2 independent experiments). Student's unpaired two-tailed t-test. (Q-R) A7r5 cells expressing comparable levels of the minimal MT-binding region of

EB3, EB3-N-LZ-GFP (green) and stained for α-tubulin (red). EB3-N-LZ-GFP localizes to MT plus-ends in NT control cells. (R) EB3-N-LZ-GFP relocalizes to the MT lattice in CLASP-depleted cells. (B-N,Q-R) Immunofluorescence. Merge zoomed region is indicated by boxed corners in Merge. White box indicates scale bar. (A-R) CLASPsi2=siRNA combination 2. See also Figure S4.

CLASP modulates microtubule-affinity and EB localization *in vitro*

To address whether CLASP independently regulates EB localization at MTs, we performed *in vitro* MT plus-end tracking assays. For these experiments, we analyzed the capacity for WT CLASP2 to remove a minimal EB1 construct, EB1N-LZ-GFP. In the absence of CLASP, this minimal EB1 construct clearly decorated the MT lattice in addition to its recruitment to MT tips (Figure 4A and 4B). Addition of 30nM WT CLASP2 during MT polymerization resulted in significant reduction of EB lattice binding (Figure 4A and 4C). In the presence of CLASP, our line scans indicated a lattice to tip ratio of 0.136 ± 0.001 compared to 0.185 ± 0.001 when EB interacted with MTs in the absence of CLASP (Figure 4D). Thus, CLASP independently modulated EB lattice localization *in vitro*. Importantly, because the minimal EB1 construct lacks the CLASP-interacting region, these data confirm our results in cells: in particular, that the observed effects are due to CLASP interactions with tubulin or MTs themselves rather than a CLASP-EB interaction.

To quantitatively analyze the effect of CLASP on EB binding, we determined EB affinity for MTs by *in vitro* binding assays utilizing MT cosedimentation. GDP-MTs were polymerized from GTP-tubulin in the presence or absence of CLASP2 then incubated with varying concentrations of EB3-GFP prior to cosedimentation. Hyperbolic fitting of the data shows that EB3-GFP has a lower affinity for GDP-MTs copolymerized WT CLASP2 when compared to GDP-MTs alone (Figure 4E and 4I). Similar to our data in cells, a CLASP2 mutant, which is unable to bind to EBs (IP12-ΔC), similarly reduced

EB3-GFP affinity for GDP-MTs (Figure 4F and 4I), confirming the result of our MT plus-end tracking assays.

In order to test whether CLASP functions during MT polymerization, we examined EB3-GFP affinity for GDP-MTs that have first been assembled then incubated with WT CLASP2; importantly, EB3-GFP affinity for these MTs did not significantly change when compared to GDP-MTs alone (Figure 4G and 4I). This reveals that CLASP must be present during MT polymerization in order to regulate EB affinity for MTs and suggests that, during polymerization, CLASPs alter the MT lattice structure thereby promoting reduced EB affinity for the lattice (model Figure 4Q).

Interestingly, using GTPγS, a slowly hydrolysable GTP analog thought to be the closest experimental model for the natural GDP-Pi state which EBs recognize, eliminated the difference between MTs polymerized with and without CLASP. Consistent with previously published reports (Maurer et al., 2011), EB3-GFP displayed higher affinity for GTPγS-MTs (Figure 4H and 4I) in comparison to GDP-MTs (Figure 4I). Co-polymerization of GTPγS-MTs with WT CLASP2 did not result in a significant reduction of EB3-GFP affinity (Figure 4H and 4I). This result indicates that CLASPs recognize or modify a particular tubulin and/or MT conformation in order to regulate MT-affinity and localization of EBs, possibly via altering the GTP-state.

GTP-tubulin content at the MT lattice is increased in CLASP-depleted cells

Because EBs have higher affinity for MT lattices formed from GTP-tubulin analogs compared to GDP-tubulin lattices (Maurer et al., 2011; Maurer et al., 2012; Zanic et al., 2009), redistribution of EBs to the MT lattice in CLASP-depleted cells could be explained by a change in GTP-tubulin content, or tubulin conformation, after CLASP-depletion. To explore this hypothesis, we took advantage of the recently described hMB11 antibody, which is thought to recognize GTP-tubulin in cells (Dimitrov et al., 2008). This antibody has been shown to recognize dynamic MT plus-ends and distinct spots along the MT lattice, referred to as GTP-tubulin remnants or GTP-tubulin islands. Currently, it is not clear whether hMB11 directly recognizes the GTP-tubulin (or GDP-P_i) conformation or a more general structural feature resembling GTP-tubulin-like states within the MT lattice. In NT control cells, hMB11 indeed highlights MT tips and occasional patches along the MT lattice (Figure 4J). Strikingly, in CLASP-depleted cells, hMB11 patches at the lattice of MTs were more abundant and extended along whole MTs in regions (Figure 4K). Quantification of GTP-tubulin fluorescence intensity revealed a statistically significant increase in CLASP-depleted cells compared to NT control (Figure 4L).

Consistent with previous findings (Dimitrov et al., 2008), the pattern of GTP-tubulin remnants along the MT lattice of CLASP-depleted cells was non-homogenous (Figure 4M) and closely resembled the speckle-like distribution of EB1 at the lattice upon CLASP-depletion (Figure 4N). Unfortunately, due to restrictions of the hMB11

antibody immunofluorescence protocol, we were unable to co-stain for EBs and GTP-tubulin in CLASP-depleted cells (similarly to what has been reported by other users of this antibody). As an alternative, we have used mathematical modeling to determine whether the EB lattice speckles and GTP-tubulin remnants are similar in size and distribution along the MT lattice. Image processing was applied to compensate for differences in contrast between EB1 and GTP-tubulin (see Supplemental Experimental Procedures). The patterns of EB1 and GTP-tubulin speckles, though not identical, had similar distribution characteristics along the MT lattice (Figure 4O and 4P); thus, these patterns could, in principle, indicate the same lattice regions. Therefore, we propose that EB lattice binding is a result of increased GTP-tubulin content along MTs in CLASP-depleted cells, and that the speckle-like appearance of EB staining reflects uneven distribution of GTP-tubulin remnants at the lattice. Because EB lattice speckles are reproducibly found along the entire MT lattice, we attribute increased GTP-tubulin lattice staining only in certain regions of the MT network to restricted hMB11 antibody sensitivity. These experiments reveal a possible mechanism for relocalization of EB proteins to the MT lattice in CLASP-depleted cells, via recognition of increased GTP-tubulin content, or another hMB11-recognized MT lattice feature.

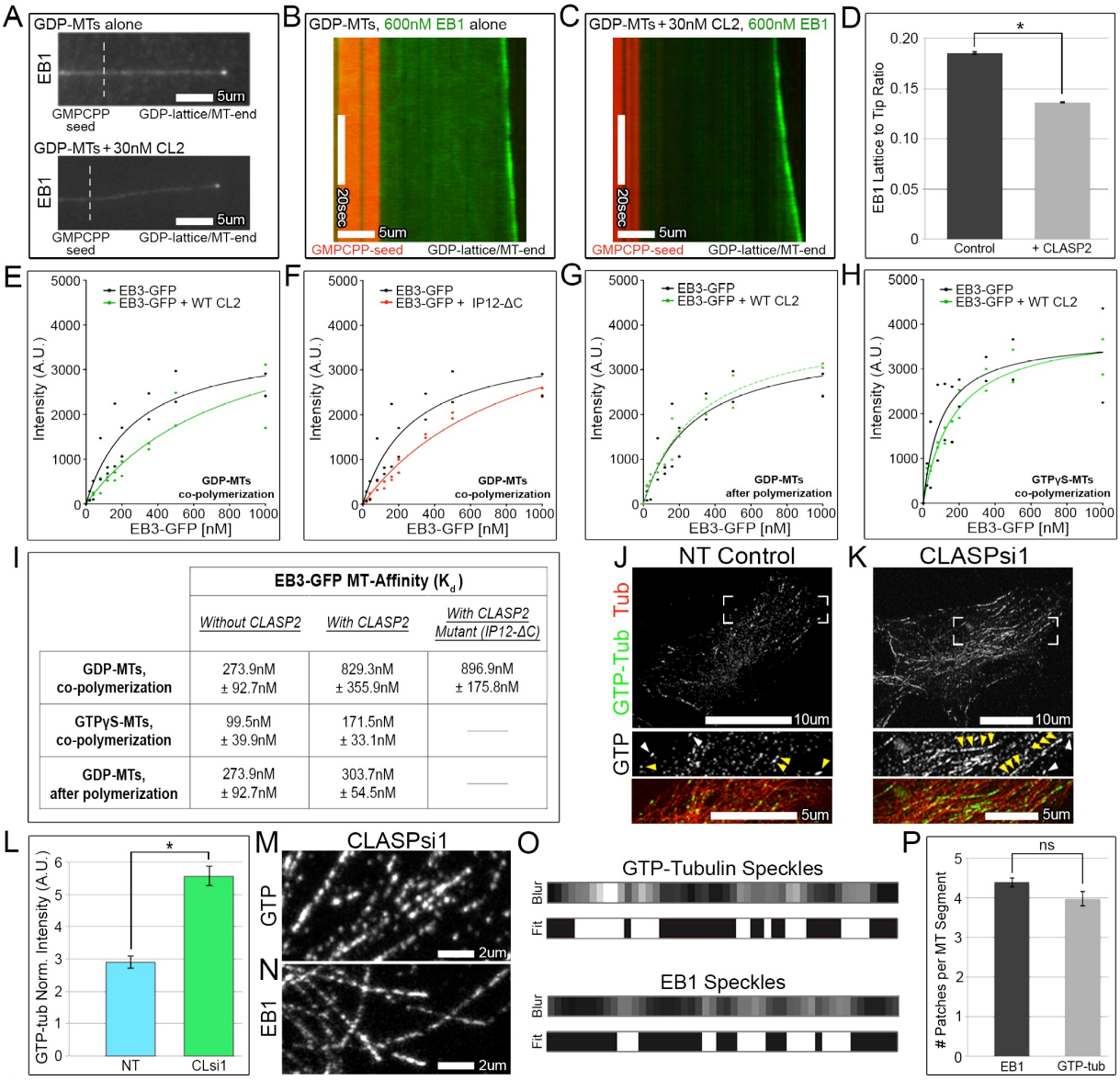

Figure 4: CLASP modulates microtubule-affinity of EB and promotes GTP-hydrolysis at microtubules *in vitro*.

Figure 4: CLASP modulates microtubule-affinity of EB and promotes GTP-hydrolysis at microtubules *in vitro*.

(A-C) *in vitro* MT plus-end tracking assays. (A) Localization of 600nM EB1N-LZ-GFP to GDP-MTs grown from GMPCPP seeds. (B,C) Kymographs of MTs (shown in A). EB1N-LZ-GFP alone (B) or in the presence of 30nM WT CLASP2 (C). Red=GMPCPP-seed, Green=EB1, CLASP2 and tubulin are unlabeled. (D) Quantification of EB1N-LZ-GFP lattice to tip ratio based on analysis from kymographs similar to (B,C). n=87 for Control, n=93 for CLASP, 2 independent experiments. Values are normalized mean intensities ± S.E.M. (E-H) Binding curves of EB3-GFP for MTs grown under various conditions: GDP-MTs polymerized in the presence of 150nM CLASP2 (E), GDP-MTs polymerized in the presence of 150nM IP12-ΔC (CLASP2 EB-binding mutant) (F), GDP-MTs in which 150nM CLASP2 was added after polymerization (G), or GTPγS-MTs polymerized in the presence of 150nM CLASP2 (H). (E-H) Intensities of MT pellet-bound EB3-GFP as a function of EB3-GFP concentration. Corresponding hyperbolic fits are shown; derived dissociation constants (K_d) are outlined in (I). (E-G) Intensities and binding curves (solid black line) for EB3-GFP bound to GDP-MTs are the same for each graph. (I) Analysis was performed over 2 independent experiments. K_d values are ± standard error. (J,K) RPE cells stained for GTP-tubulin (hMB11, grey/green) and expressing mCherry-tubulin (red). (J) In NT control cells, hMB11 localizes to GTP-tubulin at plus-ends and along the MT lattice at GTP-tubulin remnants. (K) In CLASP-depleted cells, hMB11 also localizes to plus-ends. Localization of hMB11 to GTP-tubulin remnants at

the MT lattice is extensive compared to NT control. (J,K) Merge zoomed region is indicated by boxed corners in Merge. White arrowheads=hMB11 at plus-ends, yellow arrowheads=hMB11 at GTP-tubulin remnants within MT lattice. (L) Average normalized GTP-tubulin (hMB11) intensity in NT control and CLASP-depleted cells. Based on data similar to (J,K). Values are normalized mean intensities ± S.E.M. (n=20, 2 independent experiments). (M,N) Zoomed images of RPE cells highlighting the speckled nature of GTP-tubulin (hMB11) (M) and EB1 (N) staining. (O) Binary fitting of GTP-tubulin and EB1 speckles along the MT lattice after initial blur step. (P) Quantification of number of EB1 and GTP-tubulin patches per MT segment. Based on data similar to (O). (D,L,P) Student's unpaired two-tailed t-test. Asterisks, $p<0.05$. (K,M) CLASPsi1/CLsi1 =siRNA combination 1. (J,K,M,N) Immunofluorescence. (B,C,J,K,M,N) White box indicates scale bar.

Discussion

This study has uncovered a novel regulatory mechanism for the localization and MT affinity of EB proteins. Our data indicate that, when CLASPs bind a MT, they influence the MT lattice itself to reduce EB binding along the MT, thereby promoting the characteristic EB plus-end distribution in cells. This regulation likely occurs during MT polymerization, setting up the nucleotide state of MTs sensed by EB for MT plus-end localization ((Maurer et al., 2012; Zanic et al., 2009) and others). Specifically, we show that GTP-tubulin content is increased along the lattice of CLASP-depleted cells and thus propose that the features, which become widely distributed within the MT lattice, are likely GTP-tubulin remnants that denote high-affinity binding sites for EB. Alternatively, because it is unclear as to what the GTP-tubulin antibody (hMB11) recognizes, our findings in CLASP-depleted cells may indicate that the lattice structure is altered to more closely resemble the GTP-tubulin conformation normally confined to MT plus-ends.

These findings add another level of complexity to existing evidence on the regulation of EB interactions with MTs. While CLASP clearly acts as a prominent regulator of GTP status of MTs and EB localization, in CLASP-depleted cells, EBs are still enriched at MT plus-ends in addition to their lattice localization. Also, in minimal *in vitro* MT plus-end tracking assays, EBs autonomously track MT tips and are not enriched at the lattice at physiological protein concentrations, despite CLASPs not being present in this system (Bieling et al., 2007; Buey et al., 2011; Maurer et al., 2011). In our

assays, we utilized higher concentrations of EB, which do significantly decorate the MT lattice, and this lattice localization was decreased in the presence of CLASP leading to restriction of EB binding to MT tips. This likely indicates that while GTP hydrolysis does not strictly require CLASPs, this important process is hindered in the absence of CLASPs both in cells and *in vitro*.

There are unknown differences in the lattice of MTs polymerized in cells and *in vitro* (McEwen and Edelstein, 1980; Wade and Chretien, 1993). Indeed, a recent study of MT polymerization rates demonstrates that MT properties *in vitro* only resemble those in cells when additional cellular proteins are present. Interestingly, they found that another TOG-containing MAP, XMAP215, influences EB behavior via an allosteric interaction though the MT plus-end (Zanic et al., 2013). In our study, the effect of CLASP on EB localization is TOG-domain dependent. Thus, we suggest a similar model in which CLASP allosterically regulates EB localization to MT plus-ends: as a MT polymerizes, CLASPs likely alter the MT lattice, behind the tip, by promoting GTP-hydrolysis and thus restricting high-affinity EB-binding sites to the MT plus-end. Alternatively, because CLASP is known to bind free tubulin dimers influencing their addition at MT tips during polymerization, CLASP may prime GTP-tubulin dimers for efficient hydrolysis upon incorporation into the MT lattice. Either of these mechanisms would lead to increased GTP-tubulin content at the lattice and enhanced EB lattice binding if mis-regulated.

Another potential mechanism of CLASP-dependent regulation of EB involves steric hindrance. In this scenario, under physiological conditions, CLASPs would bind the lattice during MT polymerization and remain associated with GTP-tubulin remnants, thereby blocking potential EB recruitment to these sites (and antibody recognition). In this model, CLASPs would bind MTs in a way that prevents EB-lattice interactions. Moreover, this type of MT association should be different from CLASP association with already polymerized MTs observed under overexpression conditions, in which EB is artificially recruited to MTs (Mimori-Kiyosue et al., 2005).

Because GTP-tubulin remnants are proposed to be sites of MT rescue, it is interesting that in CLASP-depleted cells MTs undergo low rescue frequency. If our model of increased GTP-tubulin content is correct, this may reflect that the absence of such a strong MT rescue factor like CLASP leads to inefficient rescues even in the presence of multiple GTP-tubulin remnants. In the steric hindrance model, the number of GTP-tubulin remnants would not actually differ in CLASP-depleted cells, and the difference in rescue activity would be explained by the absence of CLASP at these sites.

However, existing evidence leans towards the model of allosteric EB regulation by CLASPs rather than the steric hindrance model, because typically only low amounts of CLASPs are observed at the MT lattice. Furthermore, a recent study on the effects of γ-tubulin depletion reported an increase in GTP-tubulin remnants and a similar EB

distribution at MT lattices (Bouissou et al., 2014). Because γ-tubulin is a major factor defining consistency in MT structure, by controlling proper nucleation, we hypothesize that MT lattice structure in γ-tubulin depleted cells is changed, and as a result, EB lattice affinity is altered. This finding supports the idea that a structural change in the MT lattice would result in EB recruitment.

In conclusion, these findings have revealed novel functions for CLASPs, have uncovered an additional regulatory mechanism for EB plus-end tracking in cells, and have major implications for understanding the establishment of the +TIP network at MT plus-ends.

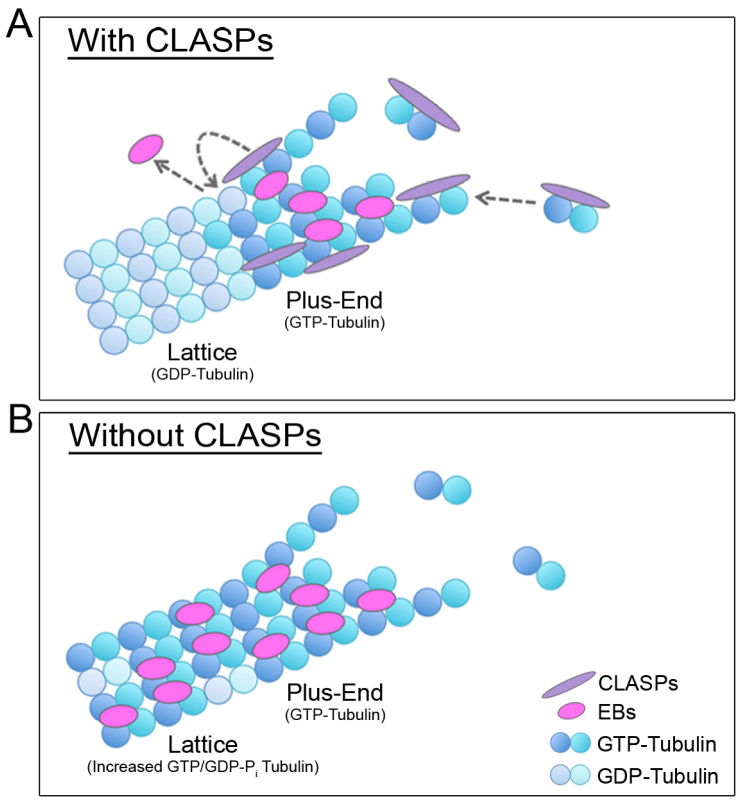

Figure 5: Model of CLASP-dependent regulation of EB localization at microtubules

Figure 5: Model of CLASP-dependent regulation of EB localization at microtubules

(A) In cells with CLASPs, EB recognizes specific features at MT tips, which are not found along the MT lattice, in addition to sensing the nucleotide state of MTs (not depicted in this model). As the MT polymerizes, CLASPs may promote hydrolysis of GTP-tubulin to restrict EB-binding sites to the plus-end. (B) In cells without CLASPs, EB-binding sites (GTP-tubulin) become widely distributed and EB localizes at MT plus-end as well as the lattice. Purple=CLASP, pink=EB, dark blue=GTP-tubulin, light blue=GDP-tubulin after hydrolysis. EB-CLASP interactions and possible steric hindrance are not shown in this model. Grey dotted-arrows indicate possible mechanisms of CLASP function during MT polymerization.

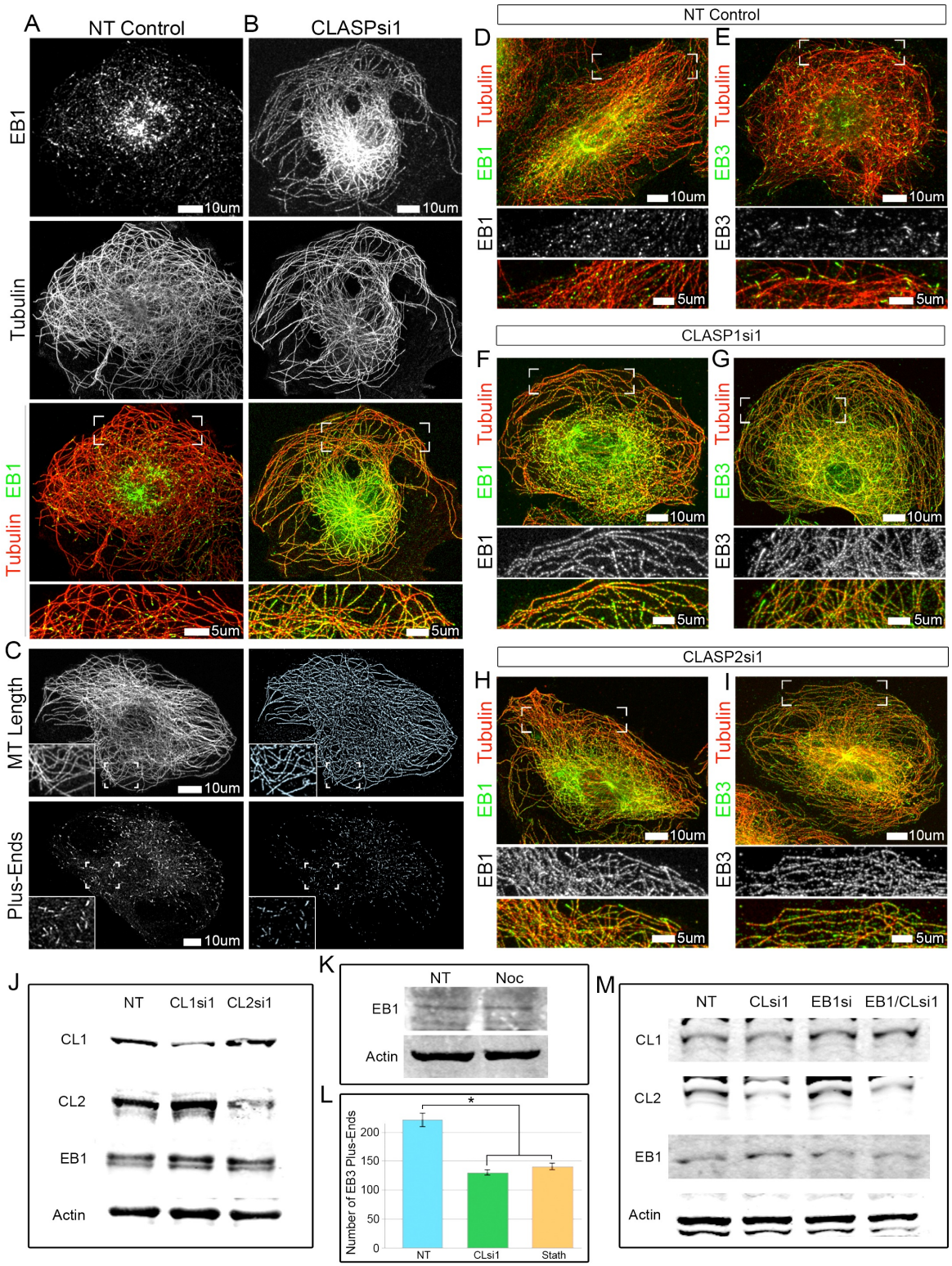

Figure S1: CLASPs 1 and 2 redundantly regulate EB localization at microtubules.

Figure S1: CLASPs 1 and 2 redundantly regulate EB localization at microtubules, related to Figure 1.

(A-B) Immunofluorescence images of A7r5 cells stained for α-tubulin (red) and EB1 (green). (A) EB3 localizes to MT plus-ends in NT control cells. (B) EB3 extensively coats the MT lattice, in addition to its normal plus-end localization, in CLASP-depleted cells. (C) Examples of Imaris MT fitting for MT length quantification (N in Figure 1) and plus-end fitting for number of EB3 plus-end quantification in (L). (D-I) Immunofluorescence images of A7r5 cells stained for α-tubulin (red) and either EB1 or EB3 (green). (D,E) EBs localizes to MT plus-ends in NT control cells. (F,G) EBs partially coat the MT lattice, in addition to their normal plus-end localization, in CLASP1-depleted cells. (H,I) Similarly, EBs partially coat the MT lattice, in addition to their normal plus-end localization, in CLASP2-depleted cells. (A-I) Merge zoomed region is indicated by boxed corners in Merge. White box indicates scale bar. (J) Western blot of A7r5 whole cell lysate showing specificity of siRNAs against CLASP1 and CLASP2. EB1 protein levels did not change in cells depleted individually of either CLASP1 or CLASP2. (K) Western blot of A7r5 whole cell lysate showing no change in EB1 protein levels upon Nocodazole treatment when compared to NT control. (L) Average number of EB3 plus-ends in NT control, CLASP-depletion, and GFP-Stathmin expression. Based on data similar to (A,B,D) in Figure 1. Values are normalized means ± S.E.M. (n=15, 3 independent experiments). Student's unpaired two-tailed t-test. Asterisks, $p<0.05$. (M) Western blot of RPE whole cell lysate showing both CLASP1 and CLASP2 protein

levels upon CLASP-depletion, EB1 protein levels upon EB1 partial depletion, and CLASPs and EB1 protein levels upon double depletion, when compared to NT control. (J,K,M) Actin was used as a loading control. (A-M) CLASPsi1/CLsi1=siRNA combination 1.

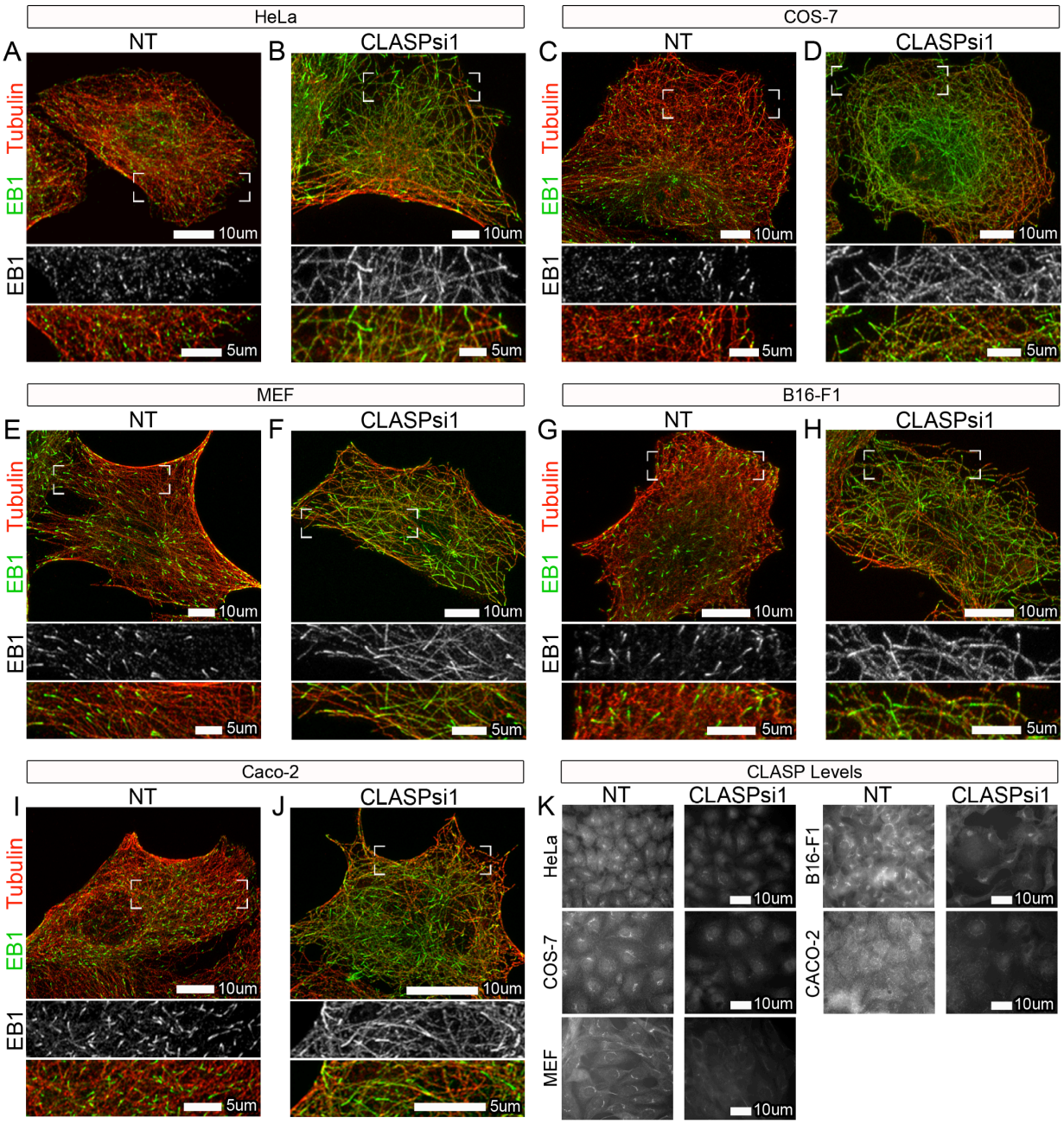

Figure S2. Altered EB localization in CLASP-depleted cells is not cell type specific.

Figure S2. Altered EB localization in CLASP-depleted cells is not cell type specific, related to Figure 1.

(A-J) Immunofluorescence images of various cell types stained for α-tubulin (red) and EB1 (green). EB1 extensively localizes to the MT lattice, in addition to MT plus-ends, in CLASP-depleted cells regardless of cell type (B,D,F,H,J), when compared to characteristic EB1 plus-end localization in NT control cells (A,C,E,G,I). (A,B) HeLa cells. (C,D) COS-7 cells. (E,F) MEF cells. (G,H) B16-F1 cells. (I,J) Caco-2 cells. (K) Representative low magnification images showing reduction in pan-CLASP levels upon CLASP-depletion in various cell types. Widefield images. (A-J) Merge zoomed region is indicated by boxed corners in Merge. (A-K) White box indicates scale bar. CLASPsi1=siRNA combination 1.

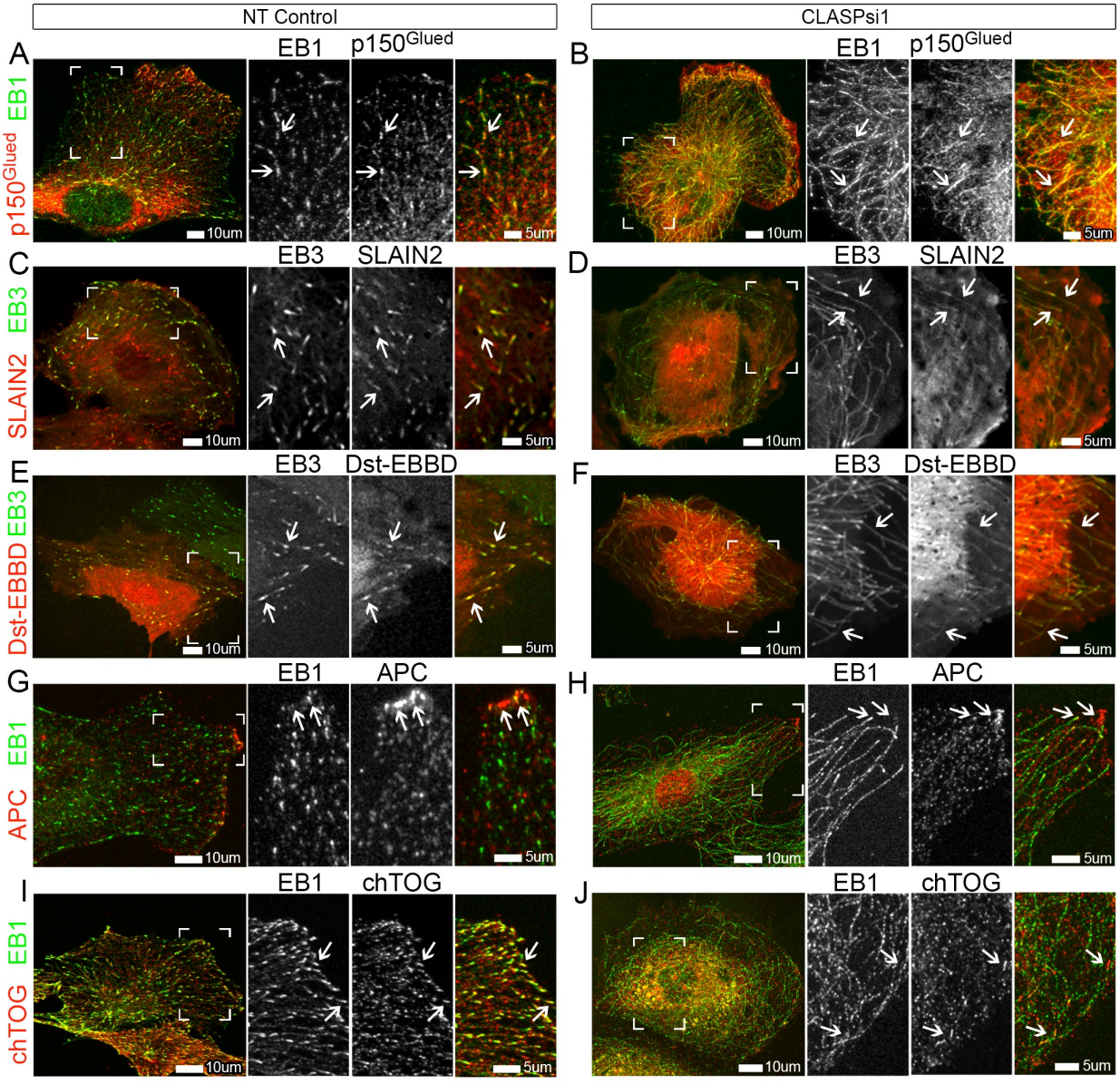

Figure S3: +TIP proteins relocalize with EBs in CLASP-depleted cells.

Figure S3: +TIP proteins relocalize with EBs in CLASP-depleted cells, related to Figure 2.

(A-D,I,J) Immunofluorescence images of RPE cells stained for EB1 or EB3 (green) and proteins representative of the major +TIP families (red) (E-H) Single confocal slice of A7r5 cells expressing tdTomato-EB3 (green) and proteins representative of the major +TIP families . (A) EB3 and $p150^{Glued}$ (CAP-Gly family) both localize to MT plus-ends in a NT control cell. (B) In addition to EB3, $p150^{Glued}$ also relocalizes to the MT lattice in a CLASP-depleted cell, as was seen for CLIP-170. (C) tdTomato-EB3 and GFP-SLAIN2 (SxIP family) both localize to MT plus-ends in a NT control cell. (D) GFP-SLAIN2 relocalizes with tdTomato-EB3 to the MT lattice in a CLASP-depleted cell. (E) tdTomato-EB3 and the minimal EB-Binding Doman of Dystonin (GFP-Dst-EBBD, SxIP family) both localize to MT plus-ends in a NT control cell. (D) In addition to tdTomato-EB3, GFP-Dst-EBBD also relocalizes to the MT lattice in a CLASP-depleted cell. (G) EB1 localizes to MT plus-ends, while APC (SxIP family) localizes to patches at the cell periphery as well as occasional MT plus-ends in a NT control cell. (H) EB1 relocalizes to the MT lattice in a CLASP-depleted cell, while APC localization upon CLASP-depletion does not differ from NT control. (E) EB1 and chTOG (EB-independent) both localize to MT plus-ends in a NT control cell. (F) EB1 relocalizes to the MT lattice in a CLASP-depleted cell, while chTOG localization upon CLASP-depletion does not differ from NT control. (A-J) Merge zoomed region is indicated by boxed corners in Merge. White

arrows indicate examples of EB/+TIP characteristic localization or lattice relocalization respectively. White box indicates scale bar. CLASPsi1=siRNA combination 1.

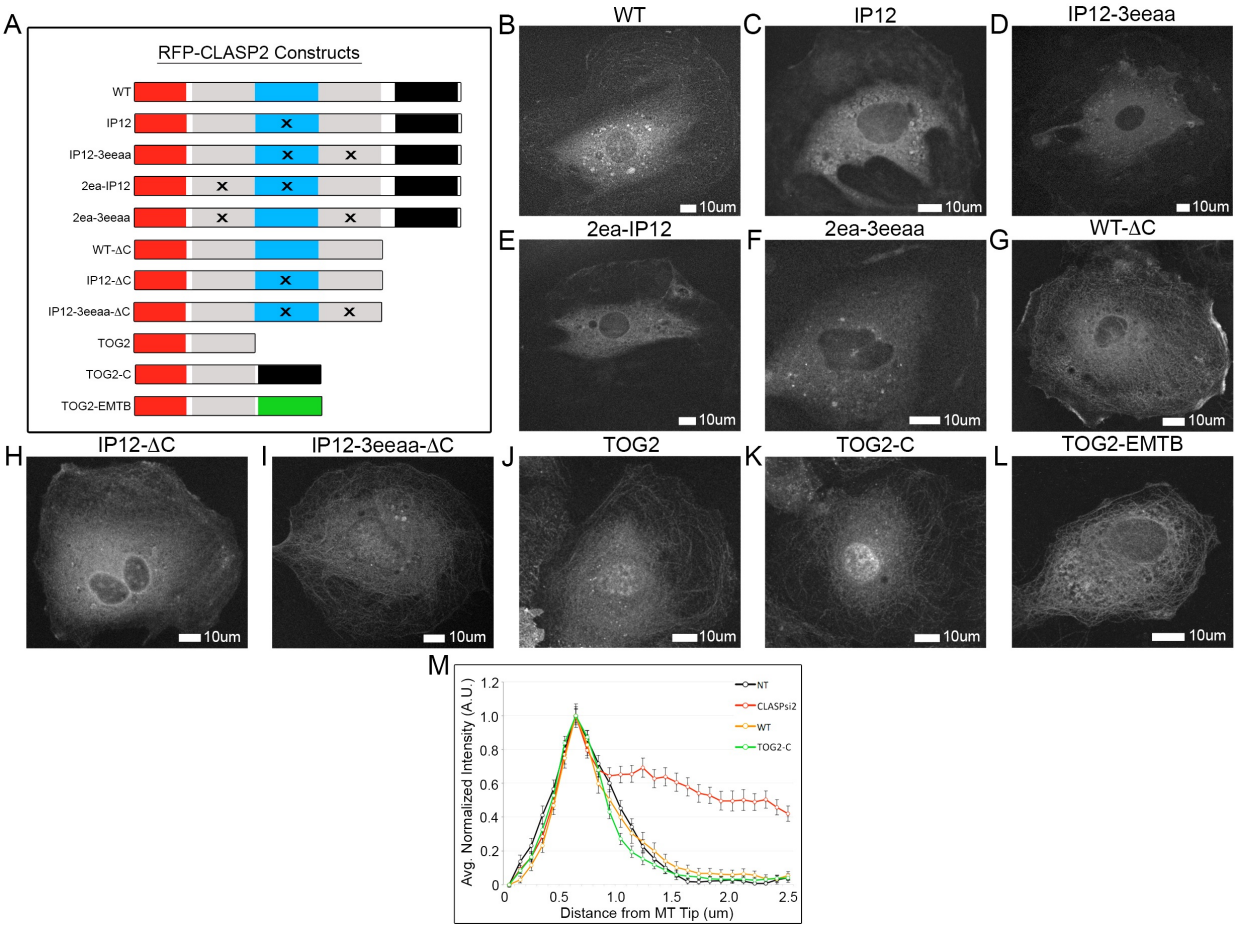

Figure S4: Localization of CLASP mutant constructs in A7r5 cells.

Figure S4: Localization of CLASP mutant constructs in A7r5 cells, related to Figure 3.

(A) Schematic representation of RFP tagged WT-CLASP2 as well as mutant CLASP2 rescue constructs. Red=RFP tag, grey=TOG-containing MT binding domains (TOG2 and TOG3), blue=EB-binding region (basic/SxIP), black=C-Terminus, and green=MT-binding domain of Ensconsin (EMTB). (B-L) Immunofluorescence. Expression of RFP-tagged CLASP2 constructs in control A7r5 cells (grey). (B) WT CLASP2 localizes to MT plus-ends. (C-F) CLASP2 mutant constructs IP12 (C), IP12-3eeaa (D), 2ea-IP12 (E), and 2ea-3eeaa (F) display low levels of MT-binding with a diffuse cytoplasmic localization. (G-L) Short CLASP2 constructs lacking the C-terminal region, WT-ΔC (G), IP12-ΔC (H), IP12-3eeaa-ΔC (I), TOG2 (J), TOG2-C (K), and TOG2-EMTB (L), displayed enhanced MT localization. (J-L) The shortest TOG2-containing CLASP2 constructs showed low levels of MT bundling, which corresponded to the level of construct expression. (B-L) White box indicates scale bar. (M) Line scan analysis quantifying rescue of normal CLIP-170 plus-end localization in CLASP-depleted cells (CLsi2=siRNA combination 2) expressing the minimal TOG2-C rescue construct. Line scan values are normalized mean intensities ± S.E.M. (n=50, 2 independent experiments).

Methods

Cells

A7r5 rat smooth muscle cells (ATCC) were maintained in low glucose (1g/L) Dulbecco's modified Eagle's medium (DMEM), without Phenol Red, supplemented with 10% fetal bovine serum (FBS). Human retinal pigment epithelial cells (hTert-RPE1, Clontech) were maintained in DMEM/F12 medium supplemented with 10% fetal bovine serum; Similarly a cherry-tubulin RPE stable line (a gift from Ryoma Ohi, Vanderbilt University, TN) was also maintained in the same media supplemented with 500ug/mL G418 antibiotic. HeLa "Kyoto" cells (a gift from Ryoma Ohi, Vanderbilt University, TN), MEF cells (a gift from Anne Kenworthy, Vanderbilt University, TN), COS-7 cells (a gift from Anne Kenworthy, Vanderbilt University, TN), and B16-F1 cells (a gift from Matthew Tyska, Vanderbilt University, TN) were maintained in DMEM medium supplemented with 10% fetal bovine serum. Caco-2 cells (a gift from Matthew Tyska, Vanderbilt University, TN) were maintained in DMEM medium supplemented with 20% fetal bovine serum. All cell types were grown in 5% CO_2 at 37°C. For experiments, cells were plated on glass coverslips coated with 10mg/ml fibronectin 72 hours prior to fixation for immunofluorescence.

Transfection, Lentiviral Infection, and Stable Lines

For transient transfection of plasmid DNA, Fugene6 (Roche) was used according to the manufacturer's protocols. For siRNA oligonucleotide transfection, HiPerFect (Qiagen) was used according to the manufacturer's protocols.

RFP-CLASP2 stable lines were generated using lentiviral constructs and were maintained in the same conditions as untreated A7r5 cells. For viral infection, supernatant containing lentiviral particles was collected from HEK293T cells transfected with lentiviral expression vectors and second generation packaging constructs (Invitrogen). A7r5 cells were infected with supernatant containing lentiviral particles with 8mg/ml polybrene overnight.

Immunofluorescence

The following mouse monoclonal primary antibodies were used: anti-α-tubulin (DM1A 1:500; Sigma); anti-EB1 (1:600, BD Transduction), anti-p150^{Glued} (1:200, BD Transduction). The following rabbit polyclonal primary antibodies were used: anti-α-tubulin (1:1000, Abcam); anti-EB3 (1:1000, a gift from A. Akhmanova); anti-CLIP-170 (1:200, a gift from Anna Akhmanova); anti-chTOG (1:1000, a gift from L. Cassimeris); anti-APC (1:1000, a gift from R. Coffey). A recombinant human primary antibody, hMB11, against GTP-MTs (1:400) was also used (a gift from F. Perez).

The following secondary antibodies were used: Alexa488, Alexa568, or Alexa647-conjugated highly cross-absorbed goat anti-mouse, goat anti-rabbit, or goat anti-Human (1:500; Invitrogen/Molecular Probes). For co-staining of MTs or chTOG with EB1/EB3, cells were fixed in cold methanol (5 min at -20°C). For co-staining of EB1/EB3 with CLIP-170/p150^{Glued}, cells were fixed in cold methanol with 1mM EGTA (20 min at -20°C) followed by 4% PFA (15min at room temperature). Staining of GTP-tubulin with

hMB11 was done according to a previously described approach (Dimitrov et al., 2008).

siRNA Depletions and Drug Treatments

Two different combinations of mixed small interfering RNA (siRNA) oligonucleotides against CLASP1 and CLASP2 were transfected into cells. Combination #1 (Dharmacon): CLASP1 siRNA targeted sequence 5'-GGATGATTTACAAGACTGG-3'; CLASP2 siRNA targeted sequence 5'-GACATACATGGGTCTTAGA-3', Combination #2 (custom design, Sigma): CLASP1 siRNA targeted sequence 5'-GCCATTATGCCAACTATCT-3'; CLASP2 siRNA targeted sequence 5'-GTTCAGAAAGCCCTTGATG-3'. Combination #2 was used for CLASP rescue experiments. Non-targeting siRNA (Dharmacon) was used as a control. Experiments were conducted 72 hours after siRNA transfection, as, at this time, minimal protein levels were detected by western blot analysis.

A small interfering RNA (siRNA) oligonucleotide against EB1 (custom design, Sigma) was transfected into cells: 5'-GACUAUGACCCUGUGGCUG-[dT]-[dT] 3'. Experiments were conducted 48 hours after siRNA transfection, as minimal protein levels were detected by western blot analysis at this time.

For MT depolymerization, cells were briefly treated with 1.5µg/mL nocodazole for 5-10min to decrease MT numbers to resemble those of CLASP-depleted cells. Alternatively, GFP-Stathmin was transfected by nucelofection according to the

manufacturer's protocol (Lonza, program X-001) and expressed at low levels for 72 hours to decrease MT numbers.

Expression Constructs

A novel mEmerald-EB3 construct was designed with an mEmerald tag on the N-terminus of EB3 and a 20 amino acid linker between mEmerald an EB3. The Emerald sequence is WT GFP with the following mutations: F64L/S65T/S72A/N149K /M153T/I167T/A206K. The Linker sequence between mEmerald and EB3 is composed of the amino acids: SGLRSGSGGGSASGGSGSGG. The EB3 sequence was cloned into an mEmerald C1 cloning vector (Clontech-style where mEmerald replaces EGFP) after amplification with the following primers:

Forward: GCCGTCAATGTGTACTCCACATCTGTGACCTCCGGACTCAGATCTGGCA GCGGTGGAGGCAGCGCATCCGGCGGAAGCGGAAGCGGGGGA

Reverse: GAGATTGAAGAGCATCAACAAGAAGACCAGGACGAGTACTAAGGATCCA CCGGATCTAG

The mEmerald-C1 cloning vector and EB3 PCR reaction were both cut with BamHI and BglII restriction enzymes, gel purified, and ligated to construct the final targeting vector.

EB3-GFP was a gift from J. Victor Small (Austrian Academy of Sciences, Austria). EB3-N-LZ-GFP, an artificial dimer of the EB3 CH MT binding domain which lacks most of the linker region, was a gift from Anna Akhmanova and has been

previously described (Komarova et al., 2009); GFP-SLAIN2 was also a gift from Anna Akhmanova (Utrecht University, Netherlands). GFP-Stathmin was kindly provided by Martin Gullberg (Umea University, Sweden). GFP-Dst-EBBD, the minimal EB-binding domain of mouse Dystonin, was cloned as an XhoI-MfeI fragment into the pEGFP-C1 vector opened with XhoI and EcoRI.

RFP tagged WT CLASP2 and CLASP2 mutants were based in the CSII-CMV-MCS lentiviral vector. CLASP2γ (60-1294aa) sequences were inserted between NdeI-NotI sites. CLASP mutant constructs contained the following point mutations: IP12 (I496A/ P497A/ I519A/ P520A), IP12-3eeaa (I496A/ P497A/ I519A/ P520A-W667E/ K833E/ R838A/ K839A), 1ea-IP12 (W106E/ K191A-I496A/ P497A/ I519A/ P520A), 2ea-3eeaa (W106E/ K191A-W667E/ K833E/ R838A/ K839A), WT-ΔC (truncated after TOG3 region with no mutations), IP12-ΔC (truncated after TOG2 region with I496A/ P497A/ I519A/ P520A mutations), IP12-3eeaa-ΔC (truncated after TOG3 domain with I496A/ P497A/ I519A/ P520A-W667E/ K833E/ R838A/ K839A mutations). TOG2 was truncated after the TOG2 region of WT CLASP2 with no mutations. TOG2-C is the same as TOG2 with the addition of a linker (residues 273-323 of Stu2) followed by the C-terminus of CLASP2γ (residues 1034-1294). TOG2-EMTB is the same as TOG2-C, but contains the MT binding region of Ensconsin (EMTB) instead of the C-terminus of CLASP2γ; EMTB was obtained by PCR from the 3xGFP-EMTB plasmid (described in (Faire et al., 1999)).

The EB protein expression constructs were based on the pET22b vector. Mouse EB3-GFP was cloned into NdeI-NotI sites of pET22b resulting in a C-terminal 6xHis-tag following the GFP. The EB1N-LZ-GFP-6xHis expression construct was made by introducing a MluI site after amino acid 139 in mouse EB1 by PCR. The leucine zipper from yeast GCN4 was then added as a MluI-BamHI fragment, followed by GFP cloned into NdeI-NotI sites of the pET22b vector.

Human CLASP2 (60-1294aa) was sub-cloned into the pET21a vector, without a stop codon, and was expressed as a C-terminal histidine-tagged protein.

Western Blotting

Western blotting was performed with the Protein Electrophoresis and Western Blotting System (Bio-Rad). For western blotting the following antibodies were used: a mouse actin antibody (1:1000; pan-Ab-5; Thermo Scientific), a rabbit actin antibody (1:1000, Sigma), a custom rabbit CLASP2 antibody (1:500; VU-83, previously described in (Efimov et al., 2007)), a rabbit CLASP1 antibody (1:500; Epitomics), a mouse EB1 antibody (1:500, BD Transduction), a mouse GFP antibody (1:500, Roche) and a guinea pig CLIP-170 antibody (1:1000, Synaptic Systems). LI-COR 800 or 700 secondary antibodies were used (LI-COR, IRDye) with an Odyssey Infrared Imaging System (LI-COR). Individual western blots were run for each +TIP protein analyzed; the actin blot shown is a representative blot.

Protein Expression and Purification

EB3-GFP-6xHis was bacterially expressed. For purification, cells were resuspended in lysis buffer (1% NP-40, 5 mM β-mercaptoethanol, protease inhibitors [1 mM PMSF; 1 mM benzamidine; and 10 μg/ml each of leupeptin, pepstatin, and chymostatin] in 1x PNI) containing 1 mg/ml lysozyme. Lysate was sonicated and clarified by centrifugation at 35,000 rpm for 1 hour in a Ti 45 rotor (Beckman). About 2 ml of Ni-NTA resin was incubated with the supernatant for 1 hour at 4°C, and then washed extensively with lysis buffer lacking NP-40 and protease inhibitors. The resin was then eluted and exchanged using a PD10 column into the final buffer (10mM K-HEPES pH 7.7, 500mM KCl, 1mM DTT), aliquoted, frozen in liquid nitrogen, and stored at - 80°C.

EB1-N-LZ-GFP-6xHis was bacterially expressed. For purification, cells were lysed by sonication in binding buffer (50mM KPO_4 pH 7.2, 400mM NaCl, 2mM $MgCl_2$, 2mM β-mercaptoethanol, 12mM imidazole) containing 0.1% Triton X-100, 1mg/ml lysozyme and 1mM PMSF. After centrifugation, the supernatant was incubated with Ni-NTA agarose, washed with binding buffer containing 20mM imidazole and eluted with 250mM imidazole. The EB1 containing fractions were loaded onto a Superdex 200 16/60 column (GE Healthcare) equilibrated with binding buffer lacking imidazole and eluted in the same buffer. Peak fractions were combined and concentrated using vivaspin columns (Sartorius), supplemented with 20% glycerol, aliquoted, frozen and stored in liquid nitrogen.

Tubulin was purified according to published protocols (Castoldi and Popov, 2003). Human CLASP2 (60-1294aa) was bacterially expressed as a C-terminal histidine-tagged protein. CLASP2 was purified using Ni-NTA Superflow, followed by HiTrapSP. The protein was eluted into elution buffer (20mM PIPES, 20nM MES, 120mM KCl, 2mM EGTA), aliquoted, frozen in liquid nitrogen, stored at - 80°C.

in vitro Microtubule-Affinity Assays and *in vitro* Plus-End Tracking Assay

For the *in vitro* MT-affinity assays, 20uM tubulin was polymerized alone or in the presence of 150nM CLASP protein (WT CLASP2 or IP12ΔC mutant) in BRB80 buffer (80 mM K-Pipes pH 6.8, 2 mM $MgCl_2$, 1 mM EGTA) supplemented with 1 mM GTP and 140 mM KCl. Samples were incubated at 37°C for 30 min, stabilized with Taxol (final concentration of 30uM) and centrifuged at 35°C for 20min at 60,000rpm. For GTPγS MTs, 1mM GTPγS was used and MTs were polymerized for 2 hours. The supernatant was subsequently removed and the MT pellets were incubated with varying concentrations of EB3-GFP (0-1000nM) for 5 min at room temperature. For experiments where CLASP protein was added after polymerization, 150nM WT CLASP2 was incubated with the MT pellet for 5 min at room temperature prior to addition of EB3-GFP protein for an additional 5 min. The MTs were then pelleted again at 35°C for 20min at 60,000rpm; supernatants and pellets were then analyzed by Sensitive Coomassie-stained SDS–PAGE.

For the *in vitro* plus-end tracking assays, preformed GMPCPP-stabilized MTs labeled with Hilyte647, were attached to a PLL-PEG-50%biotin-passivated cover slip using biotin-streptavidin linkers. With the use of a TIRF microscopy system, dynamic MTs and 600nM mEB1(1-139)-GCN4-GFP were observed in the presence of 13uM tubulin in assay buffer: 50mM KCl, 1mM GTP, 0.6mg/ml κ-casein, 0.2% methyl cellulose, 4mM DTT, 0.2mg/ml catalase, 0.4mg/ml glucose oxidase, and 50mM glucose in MRB80 (80mM PIPES, pH 6.8 with KOH, 1mM EGTA, 4mM MgCl2), supplemented with either 30nM WT CLASP2 or equal volumes of CLASP buffer as a control. A lower concentration of WT CLASP2 was used in the plus-end tracking assays to prevent strong MT bundling, which occurs at higher concentrations.

Microscopy and Image Acquisition

For acquisition of low magnification images showing relative CLASP levels, wide-field fluorescence imaging of fixed cells was performed using a Nikon 80I microscope with a Nikon Plan Fluor 40x oil lens NA 1.3 and a CoolSnap ES CCD camera (Photometrics). For all other immunofluorescence imaging, a Leica TCS SP5 confocal laser scanning microscope with an HCX PL APO 100x oil lens NA 1.47 was used to acquire confocal stacks of fixed cells.

For the *in vitro* MT plus-end tracking assays, chambers were imaged using an Olympus TIRF system (100x NA 1.49 objective with 1.6x additional magnification) and a

Hamamatsu ImageEM-1k back-illuminated EM-CCD camera under the control of xcellence software. Images were obtained every 0.5s with 200ms exposure for 100s.

Image Processing

For figure images, maximum intensity projections were made from confocal stacks. Unless otherwise indicated, all images are maximum intensity projections. Brightness and contrast were adjusted individually for each fluorescent channel and gamma settings were adjusted, when necessary, to make small structures more visible (*e.g.* +TIPs). Maximum intensity projections used for line-scan analysis and live cell movies used for FRAP analysis were unaltered.

Quantitative Analyses

Line Scan Analysis

For line scans, analysis of fluorescence intensity distribution of +TIPs along MTs in cells was performed using ImageJ software. The freehand line tool was used to draw a line (width of 3) along the length of the MT using α-tubulin staining as a guide. The point where pixel intensity abruptly changed was considered the microtubule tip. The plot profile algorithm was used to obtain fluorescence intensity values along this line. After background subtraction, line-scans were normalized via setting the average peak intensities to 1. For appropriate conditions, the average peak intensity was not normalized to 1 in order to accurately reflect decreased tip localization due to dominant negative displacement (CLIP-170 in Figure 2I and Figure 2K) or siRNA depletion (EB1 in Figure 1K). In these situations, the experimental condition's line scan was graphed proportionally to the line scan of the control by dividing both line scans by the control peak value. Lattice to Tip ratios in cells were calculated as the average normalized intensity 2um from the start of the MT (lattice) divided by the average normalized peak intensity (tip). Line-scans were acquired at random for 5 MTs per cell from 5 cells each in 2 independent experiments (total n=50). All images were taken at the same microscope settings.

For line scans analysis of EB1N-LZ-GFP fluorescence intensity along MTs *in vitro*, kymographs were first generated from rolling ball background corrected image stacks (to include the GMPCPP seed, lattice, and tip) using an ImageJ plugin

(http://biop.epfl.ch/TOOL_KYMOGRAPH.html). From these kymographs, areas of growth were identified and average EB1 intensities were measured at the tip (line width of 3) and at the lattice (rectangular ROI); These values were then used to generate the *in vitro* lattice to tip ratios. The average intensity before the tip was subtracted as background.

EB Binding Curves and Affinity

To generate binding curves for the MT-affinity analysis, the Gels tool in ImageJ was used to quantify EB3-GFP band intensity in the pellet by drawing a box of equal size around each lane. The intensity of each band was derived from the area under the resulting curves. EB levels were then normalized to the amount of total MT polymer for each reaction. The normalized pellet intensities were plotted as a function of EB3-GFP concentration. To determine the dissociation constant (K_d), Prism (GraphPad) software was used to perform a hyperbolic fit of the data using a bimolecular binding equation,

$$Y = \frac{B_{max} \cdot X}{K_d + X}$$

with K_d being the dissociation constant (as previously described in (Zhu et al., 2009)). Analysis was performed over 2 independent experiments.

Western Blot Quantification

To calculate levels of various proteins, in CLASP-depletion or other experimental conditions, western blot analysis was performed. The Gels tool in ImageJ was used to

quantify band intensities as described above. All protein levels were normalized to actin as a loading control. Analysis was performed over 3 independent experiments.

Total MT Length Quantification

Quantification of total MT length as well as number of EB plus-ends was performed using the Surfaces package in Imaris, which fits filamentous structures in the cell. For total MT length, the area of MT surfaces calculated by Imaris was divided by the apparent MT width in pixels to find the sum of the MT length. For the number of plus-ends, the same software was used to fit EB3 comets. In CLASP-depleted cells, the gamma function in ImageJ was used prior to Imaris analysis to enhance EB3 at the plus-ends of MTs (rather than the lattice); these images were then analyzed as for control. Example images of Imaris fitting can be found in Figure S1C.

GTP-Tubulin Content and Speckle Analysis

To calculate changes in levels of GTP-tubulin along MTs of CLASP-depleted cells, ImageJ was used to find the average fluorescent intensity of GTP-tubulin staining per cell, which was then averaged per condition. Because CLASP-depleted cells have decreased MT numbers, GTP-tubulin fluorescent intensity was normalized to account for changes in total MT length quantified by Imaris. All images were taken at the same microscope settings and analysis was performed over 2 independent experiments.

Analysis of EB1 and GTP-tubulin “speckle” distribution and binary fitting along MTs was performed using ImageJ and MatLab software. In brief, line scans for EB1 and GTP-tubulin were created and background was subtracted. All lines were 50 pixels in length (MT segment). To smooth EB1 speckles and highlight regions of similar fluorescent intensity, a Gaussian blur was applied (kernel radius of 1 pixel). This data was then transformed into a binary image using a relative threshold to the 25^{th} percentile: values of 0 represented no speckle, while values of 1 represented an EB1 speckle or GTP-tubulin remnant. Once binary values, runs of consecutive values equal to 1 were counted as individual EB1/GTP-tubulin patches on the MT.

Statistical Analysis

All quantitative data were collected from experiments performed in at least duplicate and are expressed as mean ± S.E.M, which were generated in Excel. Sample sizes were determined based on related previously published studies. The student's t-test (two- tailed, unpaired) was performed to determine statistical difference between two groups. A p-value of $p<0.05$ was considered statistically significant.

Acknowledgements

We thank the Kaverina, Tyska, Ohi, and Lee labs as well as MTs & Motors Club for insightful discussions. We are grateful to A. Akhmanova, L. Cassimeris, F. Perez, and R. Coffey for providing reagents used in this study. The Vanderbilt CORES facility microscopes were also instrumental in completing this work.

This study was supported by National Institutes of Health grant GM078373 (to I.K.), American Heart Association grant-in-aid 13GRNT16980096 (to I.K.), American Heart Association pre-doctoral fellowship 12PRE12040153 (to A.D.G.), and grant-in-aid for Scientific Research 22570190 (awarded to I.H.). B.P.F. is supported by the EPSRC-funded Molecular Organization and Assembly in Cells (MOAC) Doctoral Training Centre. A.S. is a Lister Institute Research Prize Fellow and this collaboration has benefited from a Strategic Partnership Grant from the University of Warwick (awarded to A.S.) and a Marie Curie Cancer Care programme grant (awarded to A.S.).

CHAPTER III

CONCULSIONS AND FUTURE DIRECTIONS

Conclusions

The study presented here contributes to a better understanding of the regulation governing the unique localization of the +TIP network. Since their initial discovery, the intriguing proteins in this network have been the focus of intense investigation. Although the exact mechanism of their plus-end localization is not yet clear, one family of proteins, the EB proteins, has been firmly established as the master regulators of the +TIP complex (Akhmanova and Steinmetz, 2008; Honnappa et al., 2009). With EBs captivating the focus of the field, the capacity for other +TIP proteins to also regulate EBs had not been addressed. Importantly, our study has begun to fill this gap in the field and has uncovered a novel regulatory mechanism for the localization and MT affinity of EBs by CLASPs. Additionally, we provide mechanistic evidence as to how CLASP likely regulates EBs at MTs. These findings add another level of complexity to the existing evidence on the regulation of EB interactions with MTs and highlight the cooperative nature of +TIP proteins.

Our data indicate that, when CLASPs bind a MT, they influence the lattice itself to reduce EB binding along the length of MTs, thereby promoting the characteristic EB plus-end distribution in cells. In cells depleted of the +TIP proteins, CLASPs, EBs

localize along the MT lattice in addition to MT tips. Notably, this phenomenon was reproducible across multiple cell types, signifying that CLASPs are authentic regulators of EBs. This altered EB localization hinted that CLASPs may be important regulators of EBs and subsequently of the entire +TIP network. EBs recruit the majority of +TIP proteins to the plus-ends of MTs where, together, they regulate MT dynamic parameters as well as play a role in numerous MT-based processes (Akhmanova and Steinmetz, 2008; Lansbergen and Akhmanova, 2006). Therefore, a drastic relocalization of EB proteins to the MT lattice in CLASP-depleted cells could have wide-reaching implications for the cell. In fact, further experiments revealed that representative proteins from the major +TIP families (CAP-Gly and SxIP) followed EBs to the MT lattice in CLASP-depleted cells, indicating that without CLASPs, the entire +TIP network is disturbed.

CLASPs are interesting members of the XMAP215/Dis1 family of proteins: they share a conventional TOG domain, but also have multiple TOG-like domains (Patel et al., 2012) and ultimately have different cellular functions (Akhmanova et al., 2001; Mimori-Kiyosue et al., 2005). Thus, it was important to understand which domains of CLASP were required to regulate EB localization at MTs. This study reveals that proper EB localization to MT tips requires the TOG2 region of CLASP (TOG-like 1), but not EB binding. The TOG-like domains of CLASPs are still quite enigmatic to the field and were recently discovered to be true TOG domains, but with a unique bent architecture (Leano et al., 2013). However, the functions of CLASP TOG-like domains are still far from

understood, especially TOG-like 2. In our studies TOG3 (TOG-like 2) was not required for CLASP-dependent regulation of EBs and suggests that there are still differences between the TOG2 and TOG3 domains of CLASPs that we do not yet understand.

The finding that CLASP MT-binding was required, but not CLASP interaction with EBs, was surprising and indicated that CLASPs may modulate MTs themselves to influence EB localization allosterically. Our data show that this regulation occurs during MT polymerization where CLASPs may set up the nucleotide state of MTs to be sensed by EBs for their plus-end localization ((Maurer et al., 2012; Zanic et al., 2009) and others). Specifically, we show that CLASP-depleted cells have increased GTP-tubulin content along their MT lattices. Thus, we propose that EB redistribution to the MT lattice in cells lacking CLASPs is due to EB recognition of widely distributed GTP-tubulin remnants (or a similar structural feature) within the MT lattice, which are normally confined to MT plus-ends.

An important aspect of this study is the *in vitro* work we have accomplished with CLASP2. The unstable nature of CLASP proteins makes their purification problematic and, as a result, has prevented widespread study of CLASPs *in vitro*. Our study is the first to incorporate full-length WT CLASP2 protein into *in vitro* assays, such as the MT plus-end tracking assays that dominate the +TIP field (Bieling et al., 2007). Importantly, our data reveal that, *in vitro*, CLASP modulates MT affinity and localization of EB in the absence of other cellular factors. The *in vitro* work in this study not only sets an example

of how CLASP can be incorporated into such experiments, but also confirms our results in cells and establishes CLASPs as direct regulators of EB proteins.

In summary, this study provides a detailed analysis of the role of CLASPs in the control of the +TIP network master regulators, EBs. This work has revealed novel functions for CLASPs while uncovering an additional regulatory mechanism for EB plus-end tracking in cells. Additionally, this CLASP-dependent regulatory mechanism has major implications for understanding the establishment of the +TIP network at MT plus-ends.

Future Directions

Clarify the mechanism of CLASP function during microtubule polymerization

Our data indicates that CLASPs function during MT polymerization to support efficient hydrolysis of GTP-tubulin and, therefore, promote exclusive EB plus-end localization. The mechanistic details of how CLASPs may function during polymerization are still unclear. *In vitro,* EB affinity assays revealed that CLASP must be present during MT polymerization in order to regulate EB affinity for MTs; however, in this assay, we are unable to determine if CLASP functions at the MT lattice or while bound to free GTP-tubulin dimers.

Hence, two models for CLASP-dependent regulation of EB localization are still plausible: 1) as a MT polymerizes, CLASPs alter the MT lattice, behind the tip, by promoting GTP-hydrolysis and thus restricting high-affinity EB-binding sites to the MT plus-end; 2) alternatively, because CLASPs are known to bind free tubulin dimers influencing their addition at MT tips during polymerization (Al-Bassam et al., 2010), CLASPs may prime these dimers for efficient GTP-hydrolysis upon incorporation into the MT lattice. Either of these mechanisms would lead to increased GTP-tubulin content at the lattice and enhanced EB lattice binding if mis-regulated.

To examine which model represents the true function of CLASPs in cells, we can start with a similar approach as in Al-Bassam et al., 2010, in which the capacity of CLASP to bind tubulin dimers was first discovered via *in vitro* MT plus-end tracking

assays. Importantly, these experiments were performed with the fission yeast CLASP homologue, Cls1p, and should be repeated with mammalian CLASP1 or CLASP2 to verify that the capacity to bind tubulin dimers is a conserved CLASP function. If this function is not conserved in mammalian CLASPs, it would suggest that our first model is more likely: CLASPs function at the MT lattice to regulate EB tip localization. If tubulin dimer binding is conserved, CLASP could act on tubulin dimers either along the MT lattice (as was shown for yeast Cls1p) or in the cytoplasm.

In experiments with cells, and with the *in vitro* MT plus-end tracking assays (proposed above), it is difficult to examine protein interactions in the cytoplasm or in the absence of MTs. To investigate if CLASP has the capacity to bind free tubulin dimers in the cytoplasm, potentially near the plus-ends of MTs, we will apply size exclusion chromatography (gel filtration). In these assays, if CLASP binds tubulin dimers, a larger complex will be formed, which migrates at a different speed than CLASP or tubulin alone (for example, as in Al-Bassam et al., 2010 and Al-Bassam et al., 2006); the stability of the complex that is formed can also be analyzed.

Previous gel filtration experiments with CLASP and tubulin have only been conducted with individual TOG domains or yeast homologues and not with full-length mammalian CLASP. In the future, it will be important to assay whether full-length CLASP, as well as the minimal construct found to rescue EB localization and modulate EB affinity *in vitro* (IP12-ΔC), is capable of binding free tubulin in gel filtration assays. It

is worth noting that fission yeast CLASP is proposed to bind tubulin dimers along the MT lattice for their incorporation into the plus-end during rescue events (Al-Bassam et al., 2010) and suggests that, in mammalian cells, a combination of our two models for CLASP-function (dimer and lattice) may be closest to what occurs in cells.

Alternatively, in the future, if enough information is known about CLASP-tubulin binding interactions, it may be possible to create a CLASP mutant that is capable of associating with the MT lattice, but that cannot bind free tubulin dimers or only binds dimers weakly. If expression of such a construct in CLASP-depleted cells does not rescue normal EB plus-end localization, this would indicate that CLASP must bind tubulin dimers to promote exclusive EB plus-end localization.

Examine the affect of CLASP on microtubule structure

Recent structural work in the field has revealed that EBs bind MTs between two protofilaments at the intersection of four tubulin dimers; this binding site is novel in comparison to other MAPs and is hypothesized to allow for EB sensing of the nucleotide state of the MT (Maurer et al., 2012). Interestingly, the positioning of EBs between protofilaments at the MT lattice also poises them to be extremely sensitive to small changes in MT lattice structure (Maurer et al., 2012). To further understand the role of CLASPs in the regulation of EB affinity and MT localization, a future direction of this project will be to analyze the structure of *in vitro* MTs formed in the absence and presence of CLASPs.

Preliminary structural studies as a part of this work did not reveal major differences between MTs copolymerized with WT CLASP2 and MTs polymerized in the absence of CLASPs (not shown). These experiments were done with negative stain EM, which is ideal for analysis of large structures, but is not optimized for the study of fine details within the MT lattice. Because MT conformation changes in the absence of CLASPs are likely to be very small differences in MT lattice structure, these initial studies were inconclusive. Moving forward, structural studies on the MT lattice in the absence of CLASP, which would create EB binding sites, should be performed with Cryo-EM Tomography (Downing and Nogales, 2010; Li et al., 2002; Maurer et al., 2012). In particular, this line of investigation would greatly benefit from a collaborator that has experience studying detailed EM of MTs (Li et al., 2002).

Additionally, if these structural studies on MT lattices are successful, it would be interesting to expand this structural work to include the study of GTP-tubulin remnant structure. In particular, how do abundant GTP-tubulin remnants upon CLASP-depletion affect the structure of MT lattices? Also, does the structure of a GTP-tubulin remnant resemble the conformation of tubulin at the plus-ends of MTs, of GTPγS-MTs, or do they represent a unique EB binding site that has yet to be characterized *in vitro* or in cells? These are important unanswered questions in the field, which could begin to be addressed by examining the structure of MT lattices that have been formed in the absence of CLASPs.

Determine if TOG domains are universal regulators of EB at microtubules

This study examines the role of CLASP2 TOG domains in the regulation of EB at MTs. CLASP2 has multiple TOG-like domains (TOG2 and TOG3), which mediate CLASP2 association with MTs (Patel et al., 2012; Slep and Vale, 2007). CLASP1 has an additional TOG1 domain and likely also has subtle differences in the structure and function of its TOG2 and TOG3 domains when compared to the analogous domains of CLASP2 (Akhmanova et al., 2001; Patel et al., 2012). In the future, it will be important to address whether the TOG2 domain of CLASP1 is also capable of regulating EB localization to the MT lattice. In addition, the TOG1 domain of CLASP1, which is a conventional TOG domain rather than a TOG-like domain, should also be tested. To address this possibility, we will perform rescue experiments in CLASP-depleted cells with various CLASP1 mutant constructs. Similarly to our experiments with the CLASP2 mutants in this study, if constructs containing specific TOG domains of CLASP1 are capable of restoring normal EB plus-end distribution, then we will conclude that CLASP1 also has the capacity to regulate EB at MTs in cells. It would also be valuable to expand upon the *in vitro* experiments with purified CLASP1 protein.

Interestingly, another +TIP protein, chTOG, also has multiple TOG domains capable of binding the MT lattice (Slep and Vale, 2007). chTOG is the mammalian family member of a conserved family of +TIP proteins that function as processive polymerases to promote rapid MT growth (Brouhard et al., 2008; Widlund et al., 2011). Although CLASPs and chTOG have different functions in cells, both protein families

contain TOG domains, and therefore it should be examined whether depletion of chTOG also alters EB localization in cells. Recent *in vitro* studies found that in the presence of XMAP215, the Xenopus chTOG homologue, EB plus-end localization was not altered; however, EB lattice localization was not investigated in these studies (Maurer et al., 2014; Zanic et al., 2013). Expanding upon these investigations will allow us to determine if the function of CLASP TOG domains is unique or if all TOG-containing proteins have the capacity to regulate EB localization and behavior at MTs. Additionally, if chTOG is not capable of regulating EBs in this manner, this would provide further evidence for the distinctive properties of the CLASP TOG-like domains.

Examine the role of CLASP in regulation of EB2

EB1 and EB3 proteins exhibit similar behavior and localization at MT in cells, while EB2 is quite different. EB2 is more dispersed along the MT lattice; however, in the absence of EB1 and/or EB3, EB2 localizes to distinct comets at MT plus-ends (Komarova et al., 2009). This suggests that EB2 is just as capable of tip tracking, but that there is competition between the EB proteins. EB2 has similar overall dimensions and arrangement of its functional domains when compared to EB1 and EB3 despite its different localization at MTs (Bu and Su, 2003; Buey et al., 2011). In control cells, endogenous EB2 binds along the MT lattice resembling EB1 and EB3 localization in CLASP-depleted cells (our preliminary data, not shown). This suggests that the subtle differences between EB2 and its family members may prevent regulation of EB2 by

CLASPs. In the future, chimeric EB proteins will be used to assess the capacity of CLASP to regulate MT lattice binding of EB1 and/or EB3 with various domains of EB2.

Confirm EB redistribution to GTP-tubulin remnants in CLASP-depleted cells

A limitation of the current study is that the GTP-tubulin antibody, due to restrictions of the immunostaining protocol, is unable to be utilized for colocalization experiments between GTP-tubulin and EBs. Assessment of GTP-tubulin content at MTs of CLASP-depleted cells revealed a significant increase in the number of GTP-tubulin remnants along the MT lattice. GTP-tubulin lattice localization was similar in distribution and appearance when compared to EB lattice staining. Moving forward, to confirm that EB redistribution in CLASP-depleted cells is to GTP-tubulin remnants within the MT lattice, we will express of a previously developed fluorescently labeled GTP-tubulin antibody in live cells (Dimitrov et al., 2008); subsequently, these cells can be staining for EB proteins using our conventional immunostaining protocol to confirm colocalization with GTP-tubulin at the MT lattice. It would also be interesting to investigate to what extend CLASP1 and CLASP2 localize to, or near, GTP-tubulin remnants in control cells.

Study the role of EB microtubule localization in disease

EB proteins are the master regulators of the +TIP complex and regulate MTs both directly and through their organizing function of this protein network at MT plus-ends (Akhmanova and Steinmetz, 2008; Komarova et al., 2009). Because MTs play an important role in many basic cellular processes, such as cell migration, cell division, and

trafficking of proteins and signaling factors, aberrant regulation of MTs and their dynamics can be catastrophic for the cell. EBs are therefore important determinants in countless cellular processes and when misregulated may result in diseases, such as cancer.

Recently, EB proteins have been implicated in the cellular response of MTs to drugs commonly used for cancer treatment and were shown to act synergistically with MT-targeting agents at MT plus-ends (Mohan et al., 2013). In the future, it will be critical to determine how altered EB localization and behavior upon CLASP-deletion may manifest in disease states in the body or differential response of patients to drug treatments. Future experiments in this study will focus on the role of EBs in cardiovascular disease, by taking advantage of our cell culture model of the vascular smooth muscle cells that line the artery wall (Louis and Zahradka, 2010).

Elucidate the role of EBs in CLASP-dependent podosome dynamics and function

Extracellular Matrix (ECM) remodeling is involved in vascular smooth muscle cell (VSMCs) infiltration into atherosclerotic plaques and is a major factor in cardiovascular disease progression. Infiltration occurs when VSMCs acquire a motile synthetic phenotype, which is triggered by extracellular stimuli; upon phenotypic transition, VSMCs gain the ability to migrate and remodel supporting ECM. This transition requires reorganization of the actin cytoskeleton, including the formation of invasive actin protrusions called podosomes (Louis and Zahradka, 2010). Normal functions of the

VSMC synthetic phenotype include vascular development and tissue repair after vascular injury (Louis and Zahradka, 2010). The invasive properties of podosomes allow infiltration of synthetic VSMCs into the artery wall during the formation of atherosclerotic plaques. Infiltration requires ECM degradation and remodeling, by secretion of degradative matrix metalloproteinases (Gimona et al., 2008), which are facilitated by podosomes *in vivo* (Quintavalle et al., 2010) and *in vitro* (Gimona et al., 2008; Kopp et al., 2006; Linder and Aepfelbacher, 2003).

Precise regulation of podosome dynamics in VSMCs is important for preventing pathogenic behavior in the artery wall. MTs regulate ECM remodeling in macrophages and osteoclasts by promoting assembly, positioning, and turnover of podosomes (Evans et al., 2003; Gil-Henn et al., 2007; Kopp et al., 2006), as well as by supporting delivery of matrix metalloproteinases to these sites (Iyemere et al., 2006). MT plus-ends directly contact podosomes, thereby regulating podosome dynamics (Kopp et al., 2006); our results show that MTs perform analogous functions in VSMCs (our unpublished results, not shown). Currently, mechanisms of the MT dynamics and MT-dependent transport essential for podosome regulation are far from understood.

Because EB proteins strongly regulate MT dynamics and MT network organization in many cell types, including VSMCs, EBs are likely to play a significant role in MT-dependent podosome regulation. As previously mentioned, our data show that in the absence of CLASPs, EB localization and affinity at MTs is altered. In addition,

CLASP-depleted VSMCs have impaired podosome formation and turnover (not shown), the effect of which may be due to altered EB binding to MTs. We hypothesize that CLASPs control the behavior of MT-binding factors, including EBs, thereby regulating podosome dynamics and function. In the future, an understanding of the mechanism whereby CLASP-dependent regulation of EBs impacts podosome dynamics will be critical and may lead to the development of therapeutic tools that manage pathological ECM remodeling and motility of VSMCs in the artery wall.

To examine the role of EBs in podosome formation, we will first deplete cells of EB1 and/or EB3 then analyze podosome formation and dynamics upon treatment with PDBu, a phorbol ester that induces podosome formation in VSMCs (Kaverina et al., 2003). In parallel, to study podosome function, we will test the capacity of EB-depleted cells to degrade ECM by performing degradation assays on fluorescent matrix substrates (Burgstaller and Gimona, 2005). If podosome formation in cells lacking EBs resembles the decreased podosome formation that we observe in CLASP-depleted cells, this will indicate that the mechanism by which CLASP regulates podosome formation is through altered EB binding to MTs.

REFERENCES

Akhmanova, A., Hoogenraad, C.C., Drabek, K., Stepanova, T., Dortland, B., Verkerk, T., Vermeulen, W., Burgering, B.M., De Zeeuw, C.I., Grosveld, F.*, et al.* (2001). Clasps are CLIP-115 and -170 associating proteins involved in the regional regulation of microtubule dynamics in motile fibroblasts. Cell *104*, 923-935.

Akhmanova, A., and Steinmetz, M.O. (2008). Tracking the ends: a dynamic protein network controls the fate of microtubule tips. Nature reviews Molecular cell biology *9*, 309-322.

Al-Bassam, J., and Chang, F. (2011). Regulation of microtubule dynamics by TOG-domain proteins XMAP215/Dis1 and CLASP. Trends in cell biology *21*, 604-614.

Al-Bassam, J., Kim, H., Brouhard, G., van Oijen, A., Harrison, S.C., and Chang, F. (2010). CLASP promotes microtubule rescue by recruiting tubulin dimers to the microtubule. Developmental cell *19*, 245-258.

Al-Bassam, J., Larsen, N.A., Hyman, A.A., and Harrison, S.C. (2007). Crystal structure of a TOG domain: conserved features of XMAP215/Dis1-family TOG domains and implications for tubulin binding. Structure *15*, 355-362.

Aldaz, H., Rice, L.M., Stearns, T., and Agard, D.A. (2005). Insights into microtubule nucleation from the crystal structure of human gamma-tubulin. Nature *435*, 523-527.

Allen, C., and Borisy, G.G. (1974). Structural polarity and directional growth of microtubules of Chlamydomonas flagella. Journal of molecular biology *90*, 381-402.

Amos, L., and Klug, A. (1974). Arrangement of subunits in flagellar microtubules. Journal of cell science *14*, 523-549.

Aylett, C.H., Wang, Q., Michie, K.A., Amos, L.A., and Lowe, J. (2010). Filament structure of bacterial tubulin homologue TubZ. Proceedings of the National Academy of Sciences of the United States of America *107*, 19766-19771.

Bieling, P., Laan, L., Schek, H., Munteanu, E.L., Sandblad, L., Dogterom, M., Brunner, D., and Surrey, T. (2007). Reconstitution of a microtubule plus-end tracking system in vitro. Nature *450*, 1100-1105.

Bouissou, A., Verollet, C., de Forges, H., Haren, L., Bellaiche, Y., Perez, F., Merdes, A., and Raynaud-Messina, B. (2014). gamma-Tubulin Ring Complexes and EB1 play

antagonistic roles in microtubule dynamics and spindle positioning. The EMBO journal *33*, 114-128.

Bratman, S.V., and Chang, F. (2007). Stabilization of overlapping microtubules by fission yeast CLASP. Developmental cell *13*, 812-827.

Brouhard, G.J., Stear, J.H., Noetzel, T.L., Al-Bassam, J., Kinoshita, K., Harrison, S.C., Howard, J., and Hyman, A.A. (2008). XMAP215 is a processive microtubule polymerase. Cell *132*, 79-88.

Bu, W., and Su, L.K. (2003). Characterization of functional domains of human EB1 family proteins. The Journal of biological chemistry *278*, 49721-49731.

Buey, R.M., Mohan, R., Leslie, K., Walzthoeni, T., Missimer, J.H., Menzel, A., Bjelic, S., Bargsten, K., Grigoriev, I., Smal, I.*, et al.* (2011). Insights into EB1 structure and the role of its C-terminal domain for discriminating microtubule tips from the lattice. Molecular biology of the cell *22*, 2912-2923.

Buey, R.M., Sen, I., Kortt, O., Mohan, R., Gfeller, D., Veprintsev, D., Kretzschmar, I., Scheuermann, J., Neri, D., Zoete, V.*, et al.* (2012). Sequence determinants of a microtubule tip localization signal (MtLS). The Journal of biological chemistry *287*, 28227-28242.

Burgstaller, G., and Gimona, M. (2005). Podosome-mediated matrix resorption and cell motility in vascular smooth muscle cells. American journal of physiology Heart and circulatory physiology *288*, H3001-3005.

Carlier, M.F., and Pantaloni, D. (1981). Kinetic analysis of guanosine 5'-triphosphate hydrolysis associated with tubulin polymerization. Biochemistry *20*, 1918-1924.

Castoldi, M., and Popov, A.V. (2003). Purification of brain tubulin through two cycles of polymerization-depolymerization in a high-molarity buffer. Protein expression and purification *32*, 83-88.

Cueva, J.G., Hsin, J., Huang, K.C., and Goodman, M.B. (2012). Posttranslational acetylation of alpha-tubulin constrains protofilament number in native microtubules. Current biology : CB *22*, 1066-1074.

Desai, A., and Mitchison, T.J. (1997). Microtubule polymerization dynamics. Annual review of cell and developmental biology *13*, 83-117.

Diamantopoulos, G.S., Perez, F., Goodson, H.V., Batelier, G., Melki, R., Kreis, T.E., and Rickard, J.E. (1999). Dynamic localization of CLIP-170 to microtubule plus ends is coupled to microtubule assembly. The Journal of cell biology *144*, 99-112.

Dimitrov, A., Quesnoit, M., Moutel, S., Cantaloube, I., Pous, C., and Perez, F. (2008). Detection of GTP-tubulin conformation in vivo reveals a role for GTP remnants in microtubule rescues. Science *322*, 1353-1356.

Downing, K.H., and Nogales, E. (2010). Cryoelectron microscopy applications in the study of tubulin structure, microtubule architecture, dynamics and assemblies, and interaction of microtubules with motors. Methods in enzymology *483*, 121-142.

Drechsel, D.N., Hyman, A.A., Cobb, M.H., and Kirschner, M.W. (1992). Modulation of the dynamic instability of tubulin assembly by the microtubule-associated protein tau. Molecular biology of the cell *3*, 1141-1154.

Efimov, A., Kharitonov, A., Efimova, N., Loncarek, J., Miller, P.M., Andreyeva, N., Gleeson, P., Galjart, N., Maia, A.R., McLeod, I.X.*, et al.* (2007). Asymmetric CLASP-dependent nucleation of noncentrosomal microtubules at the trans-Golgi network. Developmental cell *12*, 917-930.

Erickson, H.P., and O'Brien, E.T. (1992). Microtubule dynamic instability and GTP hydrolysis. Annual review of biophysics and biomolecular structure *21*, 145-166.

Etienne-Manneville, S., and Hall, A. (2003). Cdc42 regulates GSK-3beta and adenomatous polyposis coli to control cell polarity. Nature *421*, 753-756.

Evans, J.G., Correia, I., Krasavina, O., Watson, N., and Matsudaira, P. (2003). Macrophage podosomes assemble at the leading lamella by growth and fragmentation. The Journal of cell biology *161*, 697-705.

Evans, L., Mitchison, T., and Kirschner, M. (1985). Influence of the centrosome on the structure of nucleated microtubules. The Journal of cell biology *100*, 1185-1191.

Faire, K., Waterman-Storer, C.M., Gruber, D., Masson, D., Salmon, E.D., and Bulinski, J.C. (1999). E-MAP-115 (ensconsin) associates dynamically with microtubules in vivo and is not a physiological modulator of microtubule dynamics. Journal of cell science *112 (Pt 23)*, 4243-4255.

Fan, J., Griffiths, A.D., Lockhart, A., Cross, R.A., and Amos, L.A. (1996). Microtubule minus ends can be labelled with a phage display antibody specific to alpha-tubulin. Journal of molecular biology *259*, 325-330.

Gil-Henn, H., Destaing, O., Sims, N.A., Aoki, K., Alles, N., Neff, L., Sanjay, A., Bruzzaniti, A., De Camilli, P., Baron, R.*, et al.* (2007). Defective microtubule-dependent podosome organization in osteoclasts leads to increased bone density in Pyk2(-/-) mice. The Journal of cell biology *178*, 1053-1064.

Gimona, M., Buccione, R., Courtneidge, S.A., and Linder, S. (2008). Assembly and biological role of podosomes and invadopodia. Current opinion in cell biology *20*, 235-241.

Hirokawa, N., Noda, Y., Tanaka, Y., and Niwa, S. (2009). Kinesin superfamily motor proteins and intracellular transport. Nature reviews Molecular cell biology *10*, 682-696.

Hirokawa, N., Sato-Yoshitake, R., Kobayashi, N., Pfister, K.K., Bloom, G.S., and Brady, S.T. (1991). Kinesin associates with anterogradely transported membranous organelles in vivo. The Journal of cell biology *114*, 295-302.

Honnappa, S., Gouveia, S.M., Weisbrich, A., Damberger, F.F., Bhavesh, N.S., Jawhari, H., Grigoriev, I., van Rijssel, F.J., Buey, R.M., Lawera, A.*, et al.* (2009). An EB1-binding motif acts as a microtubule tip localization signal. Cell *138*, 366-376.

Hyman, A.A., Salser, S., Drechsel, D.N., Unwin, N., and Mitchison, T.J. (1992). Role of GTP hydrolysis in microtubule dynamics: information from a slowly hydrolyzable analogue, GMPCPP. Molecular biology of the cell *3*, 1155-1167.

Iyemere, V.P., Proudfoot, D., Weissberg, P.L., and Shanahan, C.M. (2006). Vascular smooth muscle cell phenotypic plasticity and the regulation of vascular calcification. Journal of internal medicine *260*, 192-210.

Kaverina, I., Stradal, T.E., and Gimona, M. (2003). Podosome formation in cultured A7r5 vascular smooth muscle cells requires Arp2/3-dependent de-novo actin polymerization at discrete microdomains. Journal of cell science *116*, 4915-4924.

Kirschner, M.W. (1978). Microtubule assembly and nucleation. International review of cytology *54*, 1-71.

Kita, K., Wittmann, T., Nathke, I.S., and Waterman-Storer, C.M. (2006). Adenomatous polyposis coli on microtubule plus ends in cell extensions can promote microtubule net growth with or without EB1. Molecular biology of the cell *17*, 2331-2345.

Kollman, J.M., Polka, J.K., Zelter, A., Davis, T.N., and Agard, D.A. (2010). Microtubule nucleating gamma-TuSC assembles structures with 13-fold microtubule-like symmetry. Nature *466*, 879-882.

Komarova, Y., De Groot, C.O., Grigoriev, I., Gouveia, S.M., Munteanu, E.L., Schober, J.M., Honnappa, S., Buey, R.M., Hoogenraad, C.C., Dogterom, M.*, et al.* (2009). Mammalian end binding proteins control persistent microtubule growth. The Journal of cell biology *184*, 691-706.

Kopp, P., Lammers, R., Aepfelbacher, M., Woehlke, G., Rudel, T., Machuy, N., Steffen, W., and Linder, S. (2006). The kinesin KIF1C and microtubule plus ends regulate podosome dynamics in macrophages. Molecular biology of the cell *17*, 2811-2823.

Kumar, P., Chimenti, M.S., Pemble, H., Schonichen, A., Thompson, O., Jacobson, M.P., and Wittmann, T. (2012). Multisite phosphorylation disrupts arginine-glutamate salt bridge networks required for binding of cytoplasmic linker-associated protein 2 (CLASP2) to end-binding protein 1 (EB1). The Journal of biological chemistry *287*, 17050-17064.

Kumar, P., Lyle, K.S., Gierke, S., Matov, A., Danuser, G., and Wittmann, T. (2009). GSK3beta phosphorylation modulates CLASP-microtubule association and lamella microtubule attachment. The Journal of cell biology *184*, 895-908.

Lansbergen, G., and Akhmanova, A. (2006). Microtubule plus end: a hub of cellular activities. Traffic *7*, 499-507.

Lansbergen, G., Grigoriev, I., Mimori-Kiyosue, Y., Ohtsuka, T., Higa, S., Kitajima, I., Demmers, J., Galjart, N., Houtsmuller, A.B., Grosveld, F.*, et al.* (2006). CLASPs attach microtubule plus ends to the cell cortex through a complex with LL5beta. Developmental cell *11*, 21-32.

Leano, J.B., Rogers, S.L., and Slep, K.C. (2013). A cryptic TOG domain with a distinct architecture underlies CLASP-dependent bipolar spindle formation. Structure *21*, 939-950.

Li, H., DeRosier, D.J., Nicholson, W.V., Nogales, E., and Downing, K.H. (2002). Microtubule structure at 8 A resolution. Structure *10*, 1317-1328.

Li, X., and Kolomeisky, A.B. (2013). Theoretical analysis of microtubules dynamics using a physical-chemical description of hydrolysis. The journal of physical chemistry B *117*, 9217-9223.

Linder, S., and Aepfelbacher, M. (2003). Podosomes: adhesion hot-spots of invasive cells. Trends in cell biology *13*, 376-385.

Lomakin, A.J., Semenova, I., Zaliapin, I., Kraikivski, P., Nadezhdina, E., Slepchenko, B.M., Akhmanova, A., and Rodionov, V. (2009). CLIP-170-dependent capture of membrane organelles by microtubules initiates minus-end directed transport. Developmental cell *17*, 323-333.

Louis, S.F., and Zahradka, P. (2010). Vascular smooth muscle cell motility: From migration to invasion. Experimental and clinical cardiology *15*, e75-85.

Lowe, J., and Amos, L.A. (1998). Crystal structure of the bacterial cell-division protein FtsZ. Nature *391*, 203-206.

Lowe, J., and Amos, L.A. (2009). Evolution of cytomotive filaments: the cytoskeleton from prokaryotes to eukaryotes. The international journal of biochemistry & cell biology *41*, 323-329.

Mallik, R., and Gross, S.P. (2004). Molecular motors: strategies to get along. Current biology : CB *14*, R971-982.

Maurer, S.P., Bieling, P., Cope, J., Hoenger, A., and Surrey, T. (2011). GTPgammaS microtubules mimic the growing microtubule end structure recognized by end-binding proteins (EBs). Proceedings of the National Academy of Sciences of the United States of America *108*, 3988-3993.

Maurer, S.P., Cade, N.I., Bohner, G., Gustafsson, N., Boutant, E., and Surrey, T. (2014). EB1 accelerates two conformational transitions important for microtubule maturation and dynamics. Current biology : CB *24*, 372-384.

Maurer, S.P., Fourniol, F.J., Bohner, G., Moores, C.A., and Surrey, T. (2012). EBs recognize a nucleotide-dependent structural cap at growing microtubule ends. Cell *149*, 371-382.

McEwen, B., and Edelstein, S.J. (1980). Evidence for a mixed lattice in microtubules reassembled in vitro. Journal of molecular biology *139*, 123-145.

McNally, F.J. (1996). Modulation of microtubule dynamics during the cell cycle. Current opinion in cell biology *8*, 23-29.

Mejillano, M.R., Barton, J.S., and Himes, R.H. (1990). Stabilization of microtubules by GTP analogues. Biochemical and biophysical research communications *166*, 653-660.

Melki, R., Carlier, M.F., Pantaloni, D., and Timasheff, S.N. (1989). Cold depolymerization of microtubules to double rings: geometric stabilization of assemblies. Biochemistry *28*, 9143-9152.

Miller, P.M., Folkmann, A.W., Maia, A.R., Efimova, N., Efimov, A., and Kaverina, I. (2009). Golgi-derived CLASP-dependent microtubules control Golgi organization and polarized trafficking in motile cells. Nature cell biology *11*, 1069-1080.

Mimori-Kiyosue, Y., Grigoriev, I., Lansbergen, G., Sasaki, H., Matsui, C., Severin, F., Galjart, N., Grosveld, F., Vorobjev, I., Tsukita, S.*, et al.* (2005). CLASP1 and CLASP2 bind to EB1 and regulate microtubule plus-end dynamics at the cell cortex. The Journal of cell biology *168*, 141-153.

Mitchison, T., and Kirschner, M. (1984a). Dynamic instability of microtubule growth. Nature *312*, 237-242.

Mitchison, T., and Kirschner, M. (1984b). Microtubule assembly nucleated by isolated centrosomes. Nature *312*, 232-237.

Mitchison, T.J. (1993). Localization of an exchangeable GTP binding site at the plus end of microtubules. Science *261*, 1044-1047.

Mohan, R., Katrukha, E.A., Doodhi, H., Smal, I., Meijering, E., Kapitein, L.C., Steinmetz, M.O., and Akhmanova, A. (2013). End-binding proteins sensitize microtubules to the action of microtubule-targeting agents. Proceedings of the National Academy of Sciences of the United States of America *110*, 8900-8905.

Nakata, T., Niwa, S., Okada, Y., Perez, F., and Hirokawa, N. (2011). Preferential binding of a kinesin-1 motor to GTP-tubulin-rich microtubules underlies polarized vesicle transport. The Journal of cell biology *194*, 245-255.

Ni, L., Xu, W., Kumaraswami, M., and Schumacher, M.A. (2010). Plasmid protein TubR uses a distinct mode of HTH-DNA binding and recruits the prokaryotic tubulin homolog TubZ to effect DNA partition. Proceedings of the National Academy of Sciences of the United States of America *107*, 11763-11768.

Nogales, E., Wolf, S.G., and Downing, K.H. (1998). Structure of the alpha beta tubulin dimer by electron crystallography. Nature *391*, 199-203.

Patel, K., Nogales, E., and Heald, R. (2012). Multiple domains of human CLASP contribute to microtubule dynamics and organization in vitro and in Xenopus egg extracts. Cytoskeleton *69*, 155-165.

Perez, F., Diamantopoulos, G.S., Stalder, R., and Kreis, T.E. (1999). CLIP-170 highlights growing microtubule ends in vivo. Cell *96*, 517-527.

Quintavalle, M., Elia, L., Condorelli, G., and Courtneidge, S.A. (2010). MicroRNA control of podosome formation in vascular smooth muscle cells in vivo and in vitro. The Journal of cell biology *189*, 13-22.

Rickard, J.E., and Kreis, T.E. (1990). Identification of a novel nucleotide-sensitive microtubule-binding protein in HeLa cells. The Journal of cell biology *110*, 1623-1633.

Roberts, A.J., Kon, T., Knight, P.J., Sutoh, K., and Burgess, S.A. (2013). Functions and mechanics of dynein motor proteins. Nature reviews Molecular cell biology *14*, 713-726.

Schlieper, D., Oliva, M.A., Andreu, J.M., and Lowe, J. (2005). Structure of bacterial tubulin BtubA/B: evidence for horizontal gene transfer. Proceedings of the National Academy of Sciences of the United States of America *102*, 9170-9175.

Schuyler, S.C., and Pellman, D. (2001). Microtubule "plus-end-tracking proteins": The end is just the beginning. Cell *105*, 421-424.

Skube, S.B., Chaverri, J.M., and Goodson, H.V. (2010). Effect of GFP tags on the localization of EB1 and EB1 fragments in vivo. Cytoskeleton *67*, 1-12.

Slep, K.C. (2009). The role of TOG domains in microtubule plus end dynamics. Biochemical Society transactions *37*, 1002-1006.

Slep, K.C., and Vale, R.D. (2007). Structural basis of microtubule plus end tracking by XMAP215, CLIP-170, and EB1. Molecular cell *27*, 976-991.

Tirnauer, J.S., and Bierer, B.E. (2000). EB1 proteins regulate microtubule dynamics, cell polarity, and chromosome stability. The Journal of cell biology *149*, 761-766.

Tran, P.T., Walker, R.A., and Salmon, E.D. (1997). A metastable intermediate state of microtubule dynamic instability that differs significantly between plus and minus ends. The Journal of cell biology *138*, 105-117.

Trinczek, B., Biernat, J., Baumann, K., Mandelkow, E.M., and Mandelkow, E. (1995). Domains of tau protein, differential phosphorylation, and dynamic instability of microtubules. Molecular biology of the cell *6*, 1887-1902.

Vale, R.D., and Fletterick, R.J. (1997). The design plan of kinesin motors. Annual review of cell and developmental biology *13*, 745-777.

Verhey, K.J., and Hammond, J.W. (2009). Traffic control: regulation of kinesin motors. Nature reviews Molecular cell biology *10*, 765-777.

Wade, R.H., and Chretien, D. (1993). Cryoelectron microscopy of microtubules. Journal of structural biology *110*, 1-27.

Walker, R.A., O'Brien, E.T., Pryer, N.K., Soboeiro, M.F., Voter, W.A., Erickson, H.P., and Salmon, E.D. (1988). Dynamic instability of individual microtubules analyzed by video light microscopy: rate constants and transition frequencies. The Journal of cell biology *107*, 1437-1448.

Weisbrich, A., Honnappa, S., Jaussi, R., Okhrimenko, O., Frey, D., Jelesarov, I., Akhmanova, A., and Steinmetz, M.O. (2007). Structure-function relationship of CAP-Gly domains. Nature structural & molecular biology *14*, 959-967.

Weisenberg, R.C., and Deery, W.J. (1976). Role of nucleotide hydrolysis in microtubule assembly. Nature *263*, 792-793.

Widlund, P.O., Stear, J.H., Pozniakovsky, A., Zanic, M., Reber, S., Brouhard, G.J., Hyman, A.A., and Howard, J. (2011). XMAP215 polymerase activity is built by combining multiple tubulin-binding TOG domains and a basic lattice-binding region. Proceedings of the National Academy of Sciences of the United States of America *108*, 2741-2746.

Wilbur, J.D., and Heald, R. (2013). Cryptic no longer: arrays of CLASP1 TOG domains. Structure *21*, 869-870.

Wittmann, T., and Waterman-Storer, C.M. (2005). Spatial regulation of CLASP affinity for microtubules by Rac1 and GSK3beta in migrating epithelial cells. The Journal of cell biology *169*, 929-939.

Zanic, M., Stear, J.H., Hyman, A.A., and Howard, J. (2009). EB1 recognizes the nucleotide state of tubulin in the microtubule lattice. PloS one *4*, e7585.

Zanic, M., Widlund, P.O., Hyman, A.A., and Howard, J. (2013). Synergy between XMAP215 and EB1 increases microtubule growth rates to physiological levels. Nature cell biology *15*, 688-693.

Zhu, Z.C., Gupta, K.K., Slabbekoorn, A.R., Paulson, B.A., Folker, E.S., and Goodson, H.V. (2009). Interactions between EB1 and microtubules: dramatic effect of affinity tags and evidence for cooperative behavior. The Journal of biological chemistry *284*, 32651-32661.